U. S. DEPARTMENT OF COMMERCE
W. Averell Harriman, Secretary
NATIONAL BUREAU OF STANDARDS
E. U. Condon, Director

AUGUST 1947
VOLUME • 39
NUMBER 2

JOURNAL OF RESEARCH

of the

NATIONAL BUREAU OF STANDARDS

Contents

RP		Page
1816.	Absorption spectra in the detection of chemical changes in cellulose and cellulose derivatives. John W. Rowen, Charles M. Hunt, and Earle K. Plyler. (Price 10 cents)	133
1817.	Anodic current efficiency in the counterflow electrolysis of uranyl chloride solutions. Walter J. Hamer. (Price 10 cents)	141
1818.	Analysis by the mass spectrometer of a liquified hydrocarbon mixture containing C_3–C_5 paraffins and olefins. Vernon H. Dibeler and Fred L. Mohler. (Price 10 cents)	149
1819.	An indentation method for measuring wear. Samuel A. McKee. (Price 10 cents)	155
1820.	Effect of magnification on the precision of indoor telescope pointing. Francis E. Washer. (Price 10 cents)	163
1821.	Heats of formation and isomerization of the eight C_8H_{12} alkylcyclohexanes in the liquid and gaseous states. Edward J. Prosen, Walter H. Johnson, and Frederick D. Rossini. (Price 5 cents)	173
1822.	Some recent advances in our understanding of the chemistry of portland cement. Robert H. Bogue. (Price 10 cents)	177

For sale by the Superintendent of Documents, U. S. Government Printing Office, Washington 25, D. C. - Price 30 cents
$4.50 per year on subscription

UNITED STATES GOVERNMENT PRINTING OFFICE, WASHINGTON : 1947

U. S. Department of Commerce
National Bureau of Standards

Research Paper RP1816
Volume 39, August 1947

Part of the Journal of Research of the National Bureau of Standards

Absorption Spectra in the Detection of Chemical Changes in Cellulose and Cellulose Derivatives *

By John W. Rowen, Charles M. Hunt, and Earle K. Plyler

The spectral absorption of thin films of cellulose acetate, regenerated cellulose, the acetate and regenerated cellulose after oxidation with nitrogen dioxide gas, and the regenerated cellulose after oxidation with periodic acid followed by chlorous acid, are recorded for the infrared from 2 to 15 microns and the ultraviolet from 215 to 400 millimicrons. The regenerated cellulose absorbed ultraviolet radiant energy only at the short wavelength end of the region studied, and there the transmittance of a film 2.8 micons thick was only slightly reduced. The acetate and oxidized celluloses absorbed in this region to a greater extent but gave no narrow absorption bands. Marked changes were observed in some of the absorption bands in the infrared region in going from cellulose acetate to regenerated cellulose and to their oxidation products. These changes were correlated with changes in the OH, CO, and COOH groups. The results indicate the possibility of estimating the amount of these groups present by spectral absorption measurements.

I. Introduction

Present-day theories regarding the chemistry and structure of cellulose, its derivatives and degradation products have been extensively studied and reviewed by several writers [1, 2, 3, 4, 5, 6].[1] However, only limited use of spectrometric measurements as a means of following the modification of cellulose by various treatments has been reported [7, 8, 9, 10]. This paper contains results of the measurement of the absorption spectra of cellulose and cellulose acetate before and after chemical treatments.

The structural formula generally assigned to cellulose is:

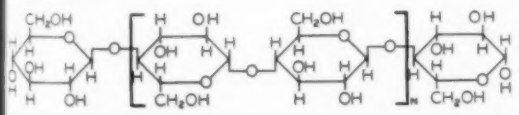

where N may take values as high as 4,500. Any sample of cellulose is considered to be made up of varying proportions of these long-chain molecules, the lengths of the individual chains depending upon the source of cellulose and its history. The greater the proportion of the short chains in a sample, the greater the number of end groups.

Cellulose is relatively unstable, and some of the linkages between atoms are ruptured, for example when cellulose is exposed to light, heat, or chemical agents. Shorter chains and additional end groups may be formed. When exposed to extreme conditions, cellulose may be degraded to relatively simple compounds.

The groups that are found in cellulose or which may be formed as a result of oxidation or cleavage include the ketone, aldehyde, hemiacetal, carboxyl, and hydroxyl groups. These groups are responsible for characteristic absorption bands in the spectra of simpler organic compounds. Not only would the bands be expected to be present in the absorption spectra of cellulose and cellulose derivatives, but the magnitude of the absorption might be a quantitative measure of the number of the groups responsible for the band.

Chemical methods for the quantitative evaluation of the groups in cellulosic materials [5, 15] sometimes lead to erroneous results because of changes in the cellulose produced by the conditions to which it is subjected during analysis. The spectrophotometric method of analysis probably would not result in appreciable change. Another way in which the spectrophotometric method could be useful is in investigating the preferential attack of reagents on specific parts of the cellulose

* Published also in Textile Research Journal, Sept. 1947.

[1] Figures in brackets indicate the literature references at the end of this paper.

molecule. For example, the oxidation of the secondary alcohol groups on carbon atoms 2 and 3 of the ring by periodic acid [11, 12] and the oxidation of the carbon atom in the 6 position to carboxyl by nitrogen dioxide gas [13, 14] could perhaps be followed spectrophotometrically.

The work reported in this paper was undertaken with this in mind.

II. Materials and Methods

The cellulose used in this study was prepared by deacetylation, in an inert nitrogen atmosphere, of cellulose acetate. The cellulose acetate was obtained in the form of yarns; it was first extracted with ether, dried, then wet with distilled water and dried again to insure complete removal of the ether. The acetate was dissolved in redistilled acetone and cast into films on a glass plate with a Bird film applicator, at room temperature. The film was then soaked from the plate with distilled water and dried.

1. Preparation of Cellulose Films

The films were deacetylated by soaking them for 24 hours in a 0.4 *M* alcoholic sodium hydroxide solution under an atmosphere of nitrogen. They were then washed with alcohol, soaked for 20 minutes in a 10-percent solution of glacial acetic acid in alcohol, again soaked for a half hour in water and then air-dried.

2. Treatment of Films with Nitrogen Dioxide (NO_2—N_2O_4)

Films of cellulose acetate and/or regenerated cellulose were suspended at room temperature, in a glass chamber that was evacuated. Dry nitrogen dioxide was then passed into the chamber. The films were left in the nitrogen dioxide atmosphere for 2 hours and then soaked for another 2 hours in distilled water with three changes of water.

3. Treatment of Films with Periodic Acid and Chlorous Acid

The films were immersed for 2 hours in a 0.042 *M* solution of periodic acid that was buffered with sodium acetate at a pH of 4.5. After contact with the periodic acid, the films were soaked for an additional 2 hours in distilled water and then washed three times with fresh distilled water. The films were then dried and subsequently transferred to a 5-percent solution of sodium chlorite buffered to a pH of 2.2 with phosphoric acid. They were allowed to remain in this solution for 2 hours. The films were then washed for 2 more hours and dried.

4. Measurement of Thickness of Films

Thickness measurements were made with a "Mikrokator" [16] that was checked against steel gage blocks calibrated by the Gage Section of the National Bureau of Standards. The standard deviation of five measurements did not exceed 0.3 μ on any spectrometer specimen. Thickness obtained in this manner with cellulose acetate films averaged 0.3 μ less than thickness based on weight, area, density calculations.

5. Measurement of Spectral Absorption in the Ultraviolet Region

The ultraviolet absorption spectrum was measured with the Beckman model DU quartz spectrophotometer [17]. The wavelength calibrations on the scale of the instrument were found to check very well against the known wavelengths of the lines of the hydrogen- and mercury-discharge tubes. It was observed in the region from about 310 to 400 mμ that when readings were made every 5 mμ, ripples appeared in the absorption pattern of these cellulosic materials. The amplitude and position of these ripples varied with the orientation of the sample in the light beam. They were interpreted as being caused by optical interference. It was possible to orient the film in the beam in such a position as to virtually eliminate them.

Figure 1 is based upon measurements made at 5 mμ intervals.

6. Measurement of Spectral Absorption in the Infrared Region

The infrared absorption spectrum was measured with a Perkin-Elmer recording infrared spectrometer with a sodium chloride prism. This type of instrument has been previously described [18]. The instrument was equipped with specially constructed gears operated by a synchronous motor for changing the wavelength, and another gear mechanism for automatically increasing the slit width in such a way as to partially compensate for the lower energy of the radiation source in the longer wavelengths. As the instrument is a single-beam spectrometer, the absorption bands of atmospheric water vapor are superimposed upon the absorption spectrum of the film under observation. The estimation of the extent of absorption by the film in this region is therefore

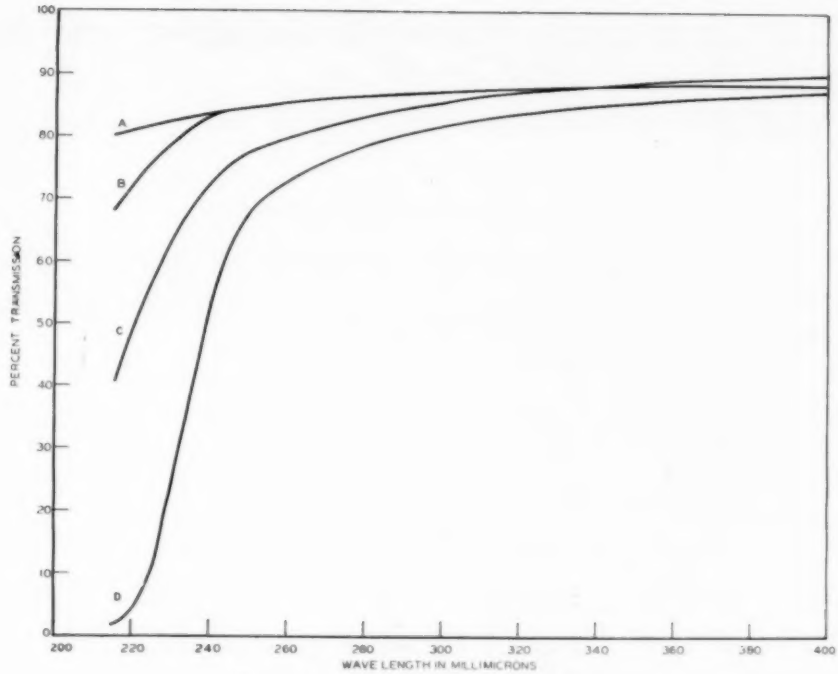

FIGURE 1.—*Ultraviolet absorption curves.*

A, Cellulose regenerated from cellulose acetate (film thickness 2.8 μ); *B*, cellulose treated with periodic acid followed by chlorous acid (film thickness 3.6 μ); *C*, ultraviolet absorption curve of cellulose acetate (film thickness 4.1 μ); *D*, cellulose treated with nitrogen dioxide gas (film thickness 3.3 μ).

ess precise than in other regions. This uncertainty has been indicated in the spectra by broken lines.

III. Results and Discussion

The infrared and ultraviolet absorption spectra of cellulose, in the oxidized and acetylated states are shown in figures 1 to 6 inclusive. The infrared spectra of these materials have in general many more bands than the ultraviolet absorption spectra. The absorption of ultraviolet light by the resonance forms of the groups of the cellulose molecule appears to take place in the energy region that is mainly below 200 mμ and hence in the vacuum region (see fig. 1). In order to properly evaluate these bands in the ultraviolet region it appears necessary to measure the absorption in the vacuum ultraviolet region as has been done for some aliphatic fatty acids [19]. It was noted that untreated cellulose had much less of a tendency to absorb short wavelength radiation than the modified celluloses as indicated in curve *A* of figure 1. Exposure of such films of cellulose to most oxidizing agents, and light resulted in an increased absorption of the short wavelengths. In many cases the absorbing agent in the cellulose created by the treatment was water soluble and showed general absorption in water. In this way it was occasionally possible to check on the extent of oxidation and contamination of the films used in this study.

The groups in cellulose containing oxidized carbon gave rise to bands in the infrared region. This spectrum was, therefore, more informative than the ultraviolet absorption spectrum. The striking alteration that accompanies deacetylation may be noted by contrasting the curves of figure 2 and figure 4. The changes in the infrared absorption spectrum of cellulose acetate that occur upon exposure to nitrogen dioxide (NO_2—N_2O_4) may be seen in figures 2 and 3. This oxidizing gas also has a marked effect on the absorption spectrum of cellulose. The effect of a somewhat arbitrary concentration of periodic acid (followed by chlorous acid) on the infrared absorption spectrum of cellulose is shown in figure 6. The bands shown in the various figures are discussed under the appropriate title as follows:

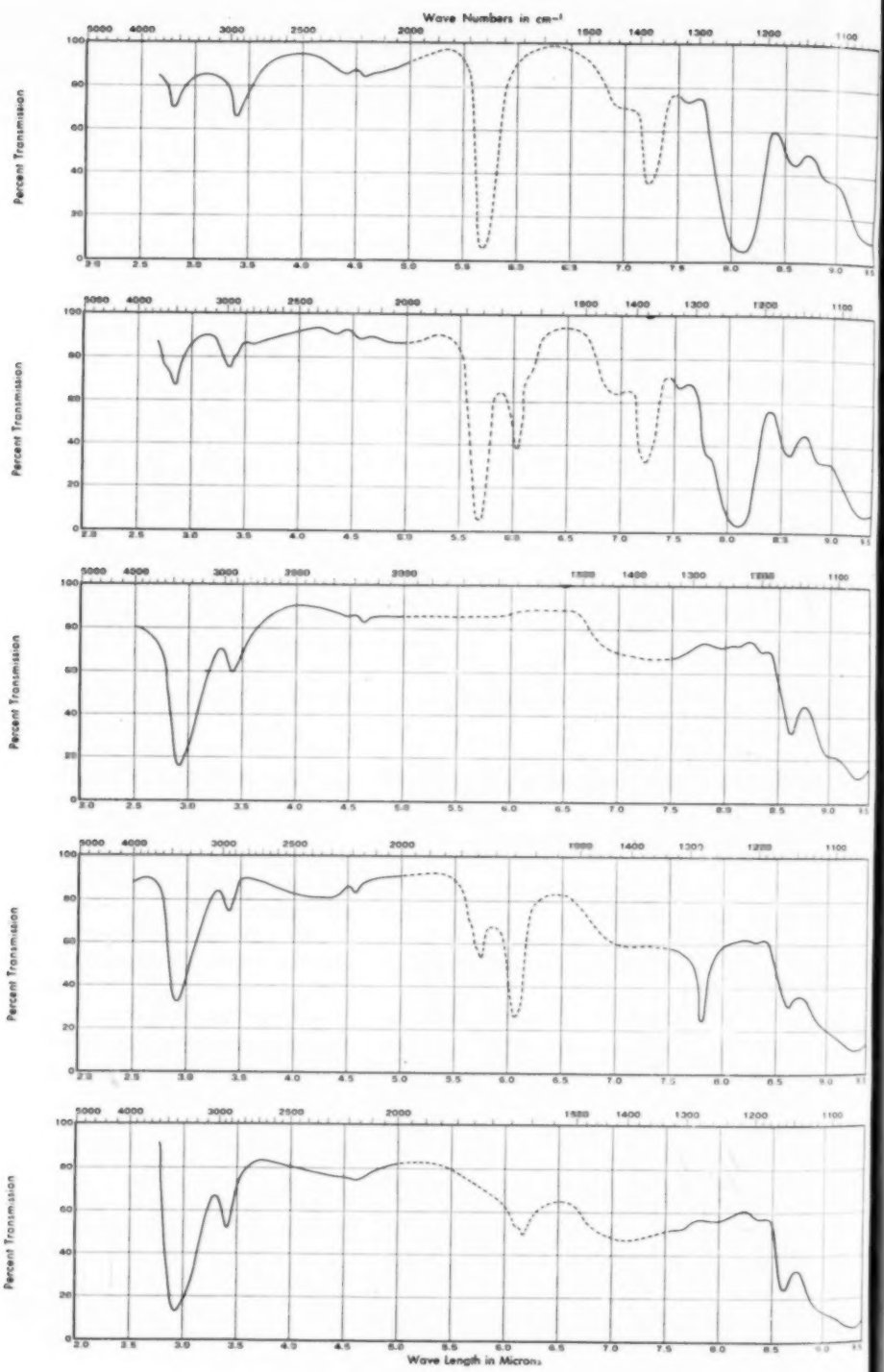
Wave Numbers in cm⁻¹
Percent Transmission
Wave Length in Microns

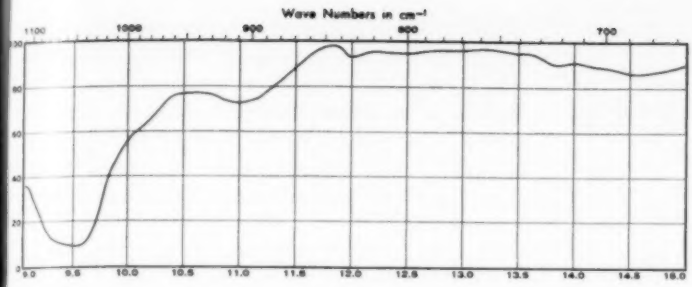

FIGURE 2.—*Infrared absorption curve of cellulose acetate (film thickness 4.1 μ).*

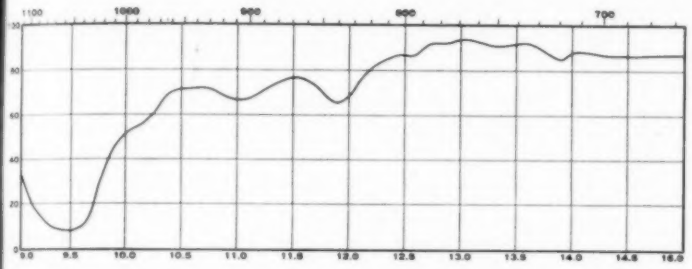

FIGURE 3.—*Infrared absorption curve of cellulose acetate exposed to nitrogen dioxide gas (film thickness 3.3 μ).*

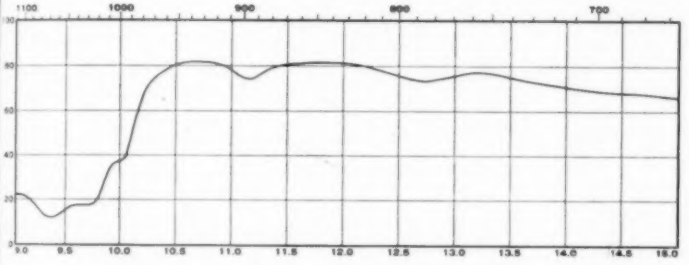

FIGURE 4.—*Infrared absorption curve of regenerated cellulose (film thickness 2.8 μ).*

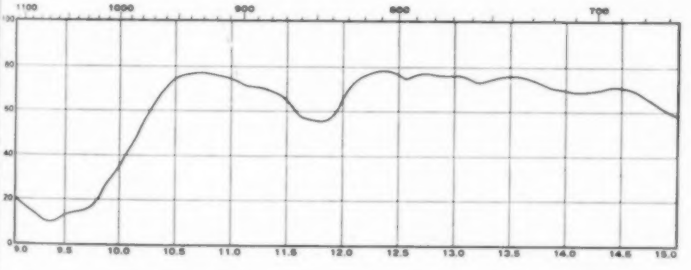

FIGURE 5.—*Infrared absorption curve of regenerated cellulose exposed to nitrogen dioxide gas (film thickness 3.3 μ).*

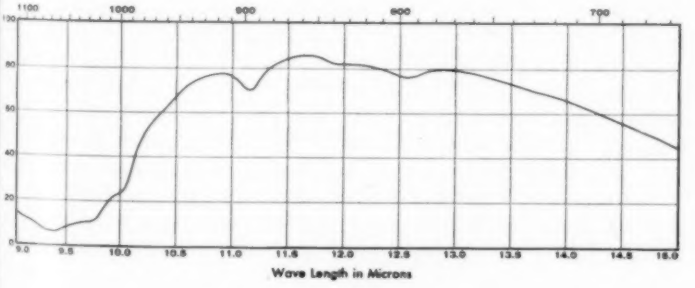

FIGURE 6.—*Infrared absorption curve of regenerated cellulose treated with periodic acid followed by chlorous acid (film thickness 3.6 μ).*

1. Cellulose Acetate

As indicated under the experimental part, the cellulose acetate was the starting point for the regeneration of the cellulose used in the study. The infrared absorption spectrum of the original cellulose acetate is shown in figure 2. This spectrum is characterized by several well-defined bands. The first band of appreciable intensity occurs at 2.8μ and is probably related to the O—H stretching vibration. The band at 3.4μ is believed to be the familiar band attributed to the C—H stretching vibration. The intense band at 5.7μ falls in the general region characteristic of the ester carbonyl group, and it shows a strong absorption in the cellulose acetate film. The band at 7.2μ is characteristic of the C—CH_3 group and hence appears in both figures 2 and 3 (untreated and nitrogen dioxide treated cellulose acetate). The intense absorption at 8.1μ is also present in curves 2 and 3. It is attributed to the ester group, as a band in this general position is always observed in the spectra of esters. These last three bands also appear in polyvinyl acetate as well as in other simpler acetates [20]. The strong band at 9.5μ is present in all the infrared absorption spectra (figures 2 to 6 inclusive) and is probably due to the C—O vibration. This vibration is very intense for methyl alcohol and is also found in polyvinyl alcohol [20].

2. Oxidized Cellulose Acetate

When cellulose acetate is oxidized with nitrogen dioxide (N_2O_4–NO_2) two new bands (fig. 3) appear in the infrared spectrum. These absorptions take place at 6.1 and 7.8 μ. The band at 7.8 μ is evident as a bulge in the side of the broad band at 8.1 μ. It will be noted later that these two bands correspond closely with the two bands that are created when cellulose is treated with nitrogen dioxide. Most organic compounds containing carboxyl groups have two strong absorption bands at approximately 6.0 and 7.8 μ. The possibility that the two bands described above might be due to carboxyl groups created by the oxidation of the unacetylated number six C—OH group will be discussed later.

3. Cellulose

When cellulose acetate is deacetylated, the marked changes that result from this process may be noted by comparing figure 2 with figure 4. One notes that the O–H vibration at 2.8 μ has become much more intense and at the same time slightly shifted to longer wavelengths. The ester carbonyl group at 5.7 μ, the CH_3 group at 7.2 and the typical ester band at 8.1 μ are all absent. On the other hand the C–O band at 9.5 μ has been considerably broadened.

4. Cellulose Oxidized With Nitrogen Dioxide

When the cellulose film is treated (as described under experimental procedure) with nitrogen dioxide, certain characteristic changes occur in the spectrum of cellulose, figure 5. First the OH absorption at 2.9 μ, seen in figure 4, is somewhat decreased in intensity. In addition, three other bands appear, the one at 5.7, one at 6.1, and a third at 7.8 μ. The band at 5.7 μ falls in the general region characteristic of the C=O group, and the other two bands are also associated with the carboxyl group as indicated under the discussion of oxidized cellulose acetate. In this work, the two strong bands at 6.1 and 7.8 μ were always associated with the oxidized cellulose believed to contain carboxyl groups.

5. Cellulose Treated With Periodic and Chlorous Acids

Exploratory experiments with the effect of periodic and chlorous acids on the infrared absorption spectrum of cellulose have been performed. Neither of these acids alone or in sequence had nearly so marked an effect on the cellulose as had nitrogen dioxide. However, a small band shown in figure 6 at 6.2 μ, not present in the spectrum of the original cellulose, was found in the treated cellulose. No definite conclusions can be drawn concerning the band until more information is available.

IV. Relationship Between Spectra and Structures

Cellulose contains over 49 percent of oxygen and this oxygen content may be expected to undergo a very small but definite increase throughout the life of the cellulose in the atmosphere. The oxidized cellulose would not be expected to be a homogeneous molecular species. In fact, one would expect the oxidized cellulose to consist of a mixture of many different kinds of oxidized cellu-

lose molecules. Workers recognizing the complexity of "oxidized" cellulose have attempted to study the effect of specific oxidizing agents on the polymer. Kenyon and coworkers have studied the oxidation of cellulose by nitrogen dioxide. They presented evidence [13, 14] that the mode of attack by this agent was highly specific. Their work indicated that the primary alcohol group on the number six carbon atom was oxidized to a carboxyl group by the oxidizing gas. The work of Jackson and Hudson [11], and Harris et al [12] indicated that periodic acid has a specific oxidizing effect on cellulose. These experiments indicate that this agent converts the secondary alcohol groups on carbons 2 and 3 to aldehyde groups in accordance with the following scheme:

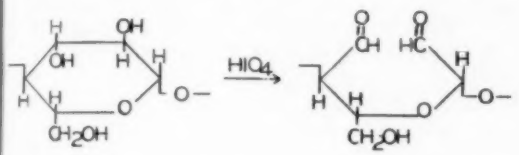

As the conditions of the reaction of nitrogen dioxide with cellulose, described under the experimental part are very similar to those employed by Kenyon et al [13, 14], it is reasonable to suppose that carboxyl groups were the primary product of the reaction. Furthermore, as adequate steps had been taken to remove any unreacted nitrogen dioxide, and as very little if any nitrocellulose would be formed under the experimental conditions, it appears reasonable to assume that the three bands present in figure 5 (the ones at 5.7, 6.1 and 7.8 μ) are all manifestations of the carboxyl group in the number six position.

Whether or not the intensities of these bands lend themselves to the quantitative estimation of carboxyl groups is not known at present. The presence of the "carboxyl" bands (5.7, 6.1, and 7.8 μ) in the spectrum of the treated cellulose acetate films (fig. 3) suggests the possibility that a good number of the primary alcohol groups (number six position) present in this material are attacked by nitrogen dioxide and converted to carboxyl groups.

The intensification of the O—H band (2.8μ) in figure 4 that accompanies deacetylation is quite striking. Presumably each acetyl group (absorption at 5.7, 7.2, and 8.1μ) is replaced by a hydroxyl group in this conversion, and the difference in intensities in the two bands (2.8 to 2.9 microns) is some measure of the number of OH groups regenerated in the process.

The effect of periodic acid, reported by other workers, was not observed in the absorption spectra of the treated cellulose in the spectral ranges studied. However, it is pointed out that these experiments may not have provided the optimum conditions for the generation of the aldehyde groups on the second and third carbon atoms. The weak band at 6.2μ in figure 6 is evidence of some reaction that did take place in these preliminary attempts.

When the cellulose acetate is converted to cellulose, and when the latter is oxidized to oxycellulose, certain fundamental aspects of the long chain molecular structure remain intact. For example, the skeletal ring-chain structure should not be profoundly altered during some of the above reaction steps. One might, therefore, expect to see manifestations of the unchanging portions of the molecule in the infrared spectrum. The absorption band at 8.6μ appears in the spectrum of all of the cellulose derivatives examined in this study. This band may be a fundamental vibration that is associated with the ring skeleton. The absorption band at 3.4μ also is common to all of the spectra, and it is undoubtedly due to the C–H stretching vibration that is characteristic of all of the compounds.

This study indicates the possibility of using the infrared absorption spectrum as a means of elucidating the alterations that may be made in the cellulose molecule.

V. Summary

1. The ultraviolet and infrared absorption spectra of cellulose, cellulose acetate, and certain oxidized samples of cellulose have been obtained.

2. Acetylation and oxidation of cellulose are reflected by profound changes in the absorption spectra of these materials.

3. This study indicates the possibility of detecting and estimating the amounts of such groups as

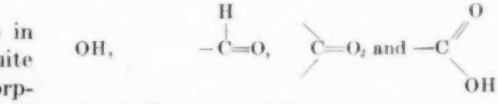

in cellulosic materials.

The authors are indebted to Lee A. Dunlap and Walter Stone for assistance in making some of the measurements reported in this paper.

VI. References

[1] Emil Ott, Cellulose and cellulose derivatives (Interscience Publishers, Inc., New York, N. Y., 1943)

[2] Emil Heuser, The chemistry of cellulose (John Wiley & Sons, Inc. New York, N. Y., 1944).

[3] G F Davidson, J. Textile Inst. **27,** 144 (1936).

[4] W. N. Haworth J. Dyers and Colourists **56,** 49 (1940).

[5] C. C. Unruh and W. O. Kenyon, Textile Research J. **16,** 1 (1946).

[6] E. Pacsu and L. A. Hiller, Textile Research J. **16,** 243 (1946).

[7] R. O. Herzog and G. Laski Z Physik Chem. **121,** 130 (1926).

[8] A. J. Wells, J. Appl. Phys. **11,** 137 (1940).

[9] G. Champetier and R. Marton, Bul Soc. Chem., France **10,** 102 (1943).

[10] Katsumoto Arsuki, and Hiroshi, Sobue. J. Soc. Chem. Ind., Japan Suppl. Binding **36,** 589B (1933)

[11] E. L. Jackson and C. S. Hudson, J. Am. Chem. Soc **59**, 2049 (1937); **60,** 989 (1938).

[12] H. A. Rutherford, F. W. Minor, A. R. Martin, and M. Harris, J. Research NBS **28,** 131 (1942) RP1491.

[13] E. C. Yackel and W. O. Kenyon, J. Am Chem. Soc. **64,** 121 (1942).

[14] C. C. Unruh and W. O. Kenyon, J. Am. Chem. Soc **64** 127 (1942).

[15] A. M. Sookne and M. Harris, Cellulose and cellulose derivatives p. 77 (Interscience Publishers, Inc., New York, N. Y., 1943).

[16] Machinery (New York) **45,** 729 (June 1939); **46,** 127 Feb. 1940)

[17] H. H. Cary and A. O Beckman, J Optical Soc. Am. **31,** 682 (1940).

[18] R. Bowling Barnes, R. S McDonald, van Zandt Williams, and R. F. Kinnaird, J. Appl. Phys. **16,** 77 (1945).

[19] J. R. Platt I. Rusoff, and H. B. Klevens, J Chem. Phys. **11,** 535 (1943).

[20] R. B. Barnes, R. C. Gore, U. Liddel, and van Z. Williams, Infrared spectroscopy (Reinhold Publishing Co., New York, N. Y., 1944).

WASHINGTON, May 6, 1947

U. S. Department of Commerce
National Bureau of Standards

Research Paper RP1817
Volume 39, August 1947

Part of the Journal of Research of the National Bureau of Standards

Anodic Current Efficiency in the Counterflow Electrolysis of Uranyl Chloride Solutions*

By Walter J. Hamer

Anodic current efficiency or the chlorine-oxygen ratio in the electrolysis of aqueous solutions of uranyl chloride was determined by a counterflow method at a temperature of 25° C. Because of the hydrolysis of dissolved chlorine, measurements were made only after sufficient time had elapsed to assure a state of equilibrium. Different concentrations of electrolyte, various electrode materials, and several current densities were employed to ascertain the effects of such changes.

The standard potentials of the oxygen and chlorine electrodes are such that oxygen should be evolved at anodes in the electrolysis of chlorides. However, chlorine is liberated because of the relative magnitudes of the oxygen and chlorine overvoltages. The value of overvoltage is dependent on the electrode material and the nature of the electrode surface. For uranyl chloride the current efficiencies increase in the order: magnetite, arc carbon, graphite, metallic carbides, and the platinum metals. Magnetite, the carbides, arc carbon, and graphite erode or pencil during electrolysis. Palladium black and platinum black become dispersed in the electrolyte. The highest current efficiency obtained was 97 percent, and the data indicated that current efficiencies of 100 percent cannot be realized for aqueous solutions of uranyl chloride at 25° C. The method is general and may be used in the determination of the current efficiency of many electrode processes. The method may also be adapted to the continuous production of gases of known purity.

I. Introduction

Current efficiency is defined as the ratio of the number of equivalents of a single electrode product to the total possible number of equivalents computed by Faraday's law of electrolysis. Deviations from Faraday's law are caused by simultaneous electrode reactions, by the interaction of anodic and cathodic products, by the diffusion of anodic and cathodic products from one electrode to another so that an electrolytic reversal of electrode processes ensues, and by the phenomena of mixed electrolytic and electronic conductance.

It is well known that current efficiencies depend on the electrode material, the current density, and to lesser extent on the concentration of the electrolyte and the temperature. It is necessary therefore to determine the current efficiency at several concentrations and obtain the current efficiency at a definite concentration by interpolation of the data. Recently, Brewer, Madorsky, and Westhaver [1] [1] described a method of electrolysis in which the concentration of the electrolyte is maintained constant throughout the electrolysis. They termed their method countercurrent electromigration. They used the method for the enrichment of the potassium isotopes utilizing the difference in the mobilities of the isotopic ions. For a successful application of the method the current efficiencies of the electrode processes must be known. It is the purpose of this paper to show how their method may be applied to the determination of the current efficiency of an electrode process, and how it may be used in the continuous production of a gas of known purity. It is illustrated with aqueous solutions of uranyl chloride. Any other

[1] Figures in brackets indicate the literature references at the end of this paper.

*This investigation was sponsored in 1942-43 by the Office of Scientific Research and Development, the National Defense Research Committee, and by the Manhattan Project. The information covered in this document will appear in volume VI, division III of the Manhattan Project Technical Series, as part of a contribution of the National Bureau of Standards.

chloride, or for that matter many other electrolytes, could be used. No studies of isotope separation were made because the formation of complex ions, the solubility of chlorine, and simultaneous electrode reactions introduce undue complications.

Upon electrolysis of a solution of uranyl chloride, the predominant reaction at the anode is

$$2\ Cl^- = Cl_2 + 2\epsilon. \quad (1)$$

Simultaneously, however, some oxygen is liberated by the reaction

$$6\ H_2O = 4\ H_3O^+ + O_2 + 4\epsilon. \quad (2)$$

The current efficiency for the production of chlorine, expressed as the chlorine-oxygen ratio in the gas liberated at the anode, was determined for solutions containing 1 equivalent of uranyl chloride in 60 moles of water (0.902 N; density at 25° C = 1.1286), in 110 moles of water (0.499 N; density at 25° C = 1.0739), and in 555.1 moles of water (0.1007 N; density at 25° C = 1.0071).[2] Electrodes of platinum, platinum black, palladium, palladium black, iridium, platinum-iridium alloy, magnetite, zirconium carbide, tungsten carbide, columbium-tantalum carbide, arc carbon, and various grades of graphite were used at a number of current densities. Loss of chlorine from the gas mixture by solution and the accompanying hydrolysis reaction

$$Cl_2 + H_2O = HClO + HCl \quad (3)$$

were prevented by electrolyzing for a sufficient time to saturate the solution with chlorine before the samples of gas generated at the anode were taken for analysis.

At the cathode the reaction

$$UO_2^{++} + 4\ H_3O^+ + 2\epsilon = U^{+IV} + 6\ H_2O \quad (4)$$

or some other type reduction occurs. This was prevented by isolating the cathode from uranyl chloride with hydrochloric acid. The hydrochloric acid formed a boundary with the solution of uranyl chloride.

II. Electrolytic Method and Drop Rates

When a solution of uranyl chloride is electrolyzed there is a loss at the anode of $t_{UO_2^{++}}$ equivalent of UO_2Cl_2 per faraday. Therefore, a more concentrated solution must be added at the anode at the proper rate to maintain constant composition of UO_2Cl_2. If no HCl had been added at the cathode there would have been a loss per faraday of t_{Cl^-} equivalent of UO_2Cl_2. When HCl is used, as is the case, there is a loss per faraday of 1 equivalent of H^+ ions owing to electrolysis, and a gain because of transference of $t_{UO_2^{++}}$ equivalent of UO_2^{++} and a loss of t_{Cl^-} equivalent of Cl^- ions. Consequently, a solution must be added at the cathode containing enough HCl to take care of the loss in HCl and enough H_2O to maintain constant the concentration of UO_2Cl_2. Also, these solutions must be added at the proper rate.

Calculations of drop rates follow: If we let

a = moles of H_2O per equivalent weight of UO_2Cl_2 in the cell,

b = moles of H_2O per equivalent weight of UO_2Cl_2 that should be added to the anode to maintain a constant composition of UO_2Cl_2 in the cell $= a(1-t_{UO_2^{++}}) = at_{Cl^-}$,

d = equivalent weight of $UO_2Cl_2 = 170.492$,

ϵ = molecular weight of $H_2O = 18.016$,

F = the faraday = 96,500 ampere-seconds,

$t_{UO_2^{++}}$ = the transference number of the UO_2^{++} ion in UO_2Cl_2,

t_{Cl^-} = the transference number of the Cl^- ion in UO_2Cl_2,

W = weight of drop in grams of a solution of UO_2Cl_2 added at the anode, we may derive the equation:

$$\frac{WF}{\text{amp}\ (d+a\epsilon t_{Cl^-})} \frac{\text{amp-sec}}{\text{drop}} = \text{anodic drop-rate}, \quad (5)$$

for the anodic drop-rate when the solution of UO_2Cl_2 is added at the rate of 1 equivalent of UO_2Cl_2 per faraday. When UO_2Cl_2 is not added at this rate we have

$$\left(\frac{a-e}{at_{UO_2^{++}}}\right)\left(\frac{WF}{\text{amp}(d+\epsilon e)}\right)\frac{\text{amp-sec}}{\text{drop}} = \text{anodic drop-rate} \quad (5a)$$

where e = moles of H_2O per equivalent weight of UO_2Cl_2 actually added to the cell.

Similarly, we may obtain the equation:

$$\frac{WF}{\text{amp}(f+a\epsilon t_{UO_2^{++}})} \frac{\text{amp-sec}}{\text{drop}} = \text{cathodic drop-rate} \quad (6)$$

[2] Densities of solutions were measured by the Lubricants and Liquid Fuels Section of the National Bureau of Standards.

for the cathodic drop-rate. Here f=moles of HCl added to the cell per faraday.

In table 1 values of the drop-rates are given for the various concentrations of UO_2Cl_2 cited in the introduction and for several values of the current. Two sets of values that will be discussed later are given for the most dilute solution. In these calculations values of 0.258, 0.283 and 0.309[3] were used for the transference number of the UO_2^{++} ion in solutions having, respectively, the normalities of 0.902, 0.499, and 0.1007.

TABLE 1.—*Drop rates for the addition of* UO_2Cl_2 *at the anode and of* HCl *at the cathode during the counterflow electrolysis of uranyl chloride* [a]

At the anode			At the cathode		
Current	Weight of drop	Drop rate	Current	Weight of drop	Drop rate
1:60 UO_2Cl_2 in cell; 1:44.5 UO_2Cl_2 added at anode; 1:15.5 HCl added at cathode					
amp	*g*	*sec/drop*	*amp*	*g*	*sec/drop*
0.3	0.0469	15.5	0.3	0.0241	24.6
.5	.0639	12.7	.5	.0422	25.8
.7	.1172	16.6	.7	.0573	25.0
1.0	.1172	11.6	1.0	.0573	17.6
1:110 UO_2Cl_2 in cell; 1:78.9 UO_2Cl_2 added at anode; 1:31.1 HCl added at cathode					
0.3	0.0600	13.6	0.3	0.0462	24.9
.5	.1103	15.0	.5	.0650	21.0
1:555.1 UO_2Cl_2 in cell; 1:383.5 UO_2Cl_2 added at anode; 1:171.5 HCl added at cathode					
0.1	0.0481	6.5	0.1	0.0480	14.9
.2	.0751	5.1	.2	.0480	7.4
1:555.1 UO_2Cl_2 in cell; 1:60 UO_2Cl_2 added at anode; 1:171.5 HCl added at cathode					
0.1	0.0193	42.9	0.1	0.0480	14.9
.2	.0254	28.3	.2	.0480	7.4

[a] The rates given in the table are calculated from theoretical principles. In practice, owing to fluctuations in the room temperature, the rates varied somewhat from those given in the table. Also, for current efficiencies considerably below 100 percent, the rates were somewhat different than the theoretical. For example, the rate for the 1:60 solution at a current of 0.5 amp is 12.7 sec/drop. At the beginning the rate was 12.7 and was changed to 12.5 within 7 hr and to 12.0 within an additional 5 hr, for platinum anodes. This represents an extreme case wherein there was a definite shift. In general, the rates increased and decreased around the theoretical value over a period of time.

[3] These values were interpolated from the combined data of E. R. Smith and H. Matheson (National Bureau of Standards, Washington, D. C. Jan. 28, 1942), of D. A. MacInnes and Associates (Rockefeller Institute for Medical Research, New York City, April 2, 1942), and of C. A. Kraus and Associates (Brown University, Providence, R. I., Oct. 26, 1942).

III. The Electrolytic Cell and Procedure

A schematic diagram of the electrolytic cell with auxiliary parts is shown in figure 1. The cell consisted of a cathode compartment, A, and an anode compartment, B, separated by a glass wool frit, I,

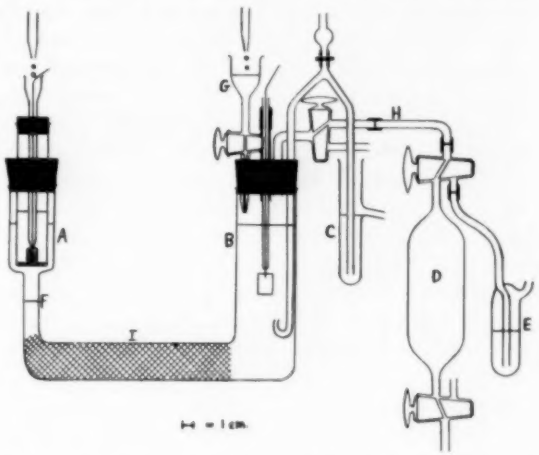

FIGURE 1.—*Schematic diagram of the electrolytic cell and gas-sampling pipette with auxiliary equipment.*

to prevent diffusion of electrolytic products from one electrode to another. The cell was placed in a water bath to facilitate rapid-heat conduction from the packed tube. The cell was first filled with a solution of UO_2Cl_2 (1:60) to the level marked, F. A solution of HCl, 15 percent more dilute than the 1:15.5 solution added at the cathode, was carefully poured into the cathode compartment to form a boundary with the solution of UO_2Cl_2, and enough solution of UO_2Cl_2 added at the anode to fill the cell.

The electrolysis was then started and a 1:44.5 solution of UO_2Cl_2 was added dropwise to the anode and a 1:15.5 solution of HCl likewise to the cathode both at the proper rate. A 115-v direct current line was used as the source of electrical power. In the majority of the experiments a current of 0.5 amp was used. In some, a current of 0.3, 0.7, or 1.0 amp was employed, drop rates being adjusted accordingly.

The anode compartment was made air tight. The solution of UO_2Cl_2 was introduced through funnel, G, carrying a stopcock to prevent air from being drawn into the anode compartment and to prevent escape of the chlorine-oxygen mixture to the atmosphere. A glass tube with stopcock as

shown led from the anode compartment to a gas sampling pipette, D, of about 200-ml capacity, adapted with a trap, E, containing 1:60 UO_2Cl_2 solution.

As electrolysis proceeded, the chlorine formed at the anode escaped through the tube leading to the pipette and also pushed solution out through the overflow. The pH of the overflow solution, C, was measured with a Beckman pH-meter at frequent intervals during the electrolysis. The initial pH of 1.44 decreased gradually within 3 hours to 1.38 and thereafter remained constant at 1.38, indicating that the solution in the anode compartment had become saturated with chlorine gas. When the pH of the overflow had attained an equilibrium value, the gas in the anode was permitted to flow for about one-half hour (228 ml of Cl_2 are evolved per hour at 25° C and 1 atm at a current of 0.5 amp) through tube, H, and trap, E, to flush out all the confined air. Then samples were drawn into the evacuated pipette, D, at a very slow rate. For all the determinations, 1½ to 2 hours were taken to fill the pipette. As the gas was drawn into the pipette, the solution in the overflow (Cl_2 saturated) was drawn into the anode compartment. The pipette stopcock was then closed, solution was forced out of the anode compartment into the overflow by the generated gas and the added solutions, and the procedure repeated approximately 22 times at intervals from 4 to 5 minutes (volume of the overflow cup was about $\frac{1}{22}$ of the volume of the pipette; 22 fillings being required). An indication of the pressure of chlorine-oxygen mixture in the pipette was given by the head of the overflow solution; when no flow of gas occurred it was known that the pipette was filled with gas.

The gas collected in the pipette was analyzed by absorption in a 1.0 N solution of KOH, which rose from a beaker into the pipette as the chlorine dissolved. Corrections were made for the air contained in the entrance tube for KOH, and the pressure of the residual gas (oxygen) that did not dissolve was corrected to 1 atmosphere pressure, using the recorded barometric pressure and the difference in the heights of the two KOH levels. The total volume of gas and the volume of Cl_2 were determined from the known weights of the pipette, the pipette filled with water, and pipette containing the various amounts of KOH. The density of the KOH solution was determined with the pipette in like manner.

In the above, the procedure was described for the electrolysis of a 1:60 solution of UO_2Cl_2. The procedure for the electrolysis was the same for the more dilute solutions with exception of the 0.1007 N solution. In the first experiment a 1:383.5 solution of UO_2Cl_2 and a 1:171.5 solution of HCl were added, respectively, to the anode and cathode compartments. However, it was found that the rates of addition of these solutions were nearly equal to the rates of evolution of and subsequent saturation of the solution with Cl_2, so that nearly all the evolved Cl_2 was lost in maintaining equilibrium. Consequently, attainment of equilibrium was exceedingly slow. In later experiments, therefore, a 1:60 solution of UO_2Cl_2 was added at the anode at a slower rate calculated by eq 5a. Attainment of equilibrium was then more rapid.

Another factor had to be considered. Above it was stated that a solution of HCl, 15 percent more dilute than that added at the cathode, was used in forming the boundary. This was necessary to assure a sharp boundary between the solutions of HCl and UO_2Cl_2. The concentration of HCl required is given by the regulating function of Kohlrausch [2]:

$$\frac{C_{H^+}}{t_{H^+}} = \frac{C_{UO_2^{++}}}{t_{UO_2^{++}}} \tag{7}$$

where C represents the equivalent concentration of the ions denoted by subscripts. For 1:15.5, 1:31.1, and 1:171.5 solutions of HCl, the transference number of the H^+ ion is, respectively, 0.844, 0.838, and 0.832 [4]. Consequently, the normality of HCl for use with solutions of UO_2Cl_2 of normality 0.902, 0.499, and 0.1007 must be, respectively, 2.95, 1.49, and 0.271. Consequently, the 1:15.5, 1:31.1, and 1:171.5 solutions of HCl were made 15 percent more dilute with water (densities of HCl solutions from reference [3]). A closer adjustment of the concentration was not necessary. Theoretically, it would appear that any concentration of HCl could be used because of an automatic adjustment of the speed of the ions arising from variable potential gradients at the junction. However, MacInnes and Smith [5] have shown experimentally that the concentrations of the two solutions in contact must conform to eq 7 within about 10 percent. The 15-percent

dilution is well within this limit. Furthermore, owing to the hydrolysis of UO_2Cl_2 and dissolved Cl_2, some hydrogen ions migrate across the boundary between HCl and UO_2Cl_2 under the influence of the electric field. In practice the boundary was steady, slight adjustments being made from time to time in the cathodic drop-rate when the boundary showed a tendency to move toward or away from the cathode. For the present purpose the adjustment of the boundary was adequate.

IV. Current Efficiencies

In tables 2 and 3 the current efficiencies (percentage yield of Cl_2) are given for different electrode materials at several current densities and for various concentrations of UO_2Cl_2. The precision of the method is illustrated by data given in table 4. The precision of the method is high and of the order of 0.1 to 0.2 percent. The current efficiencies obtained in this way are higher than those obtained by the usual methods, in which insufficient time is allowed to assure equilibrium between the gas and liquid phases. In table 5 some data are given to show the effects of time of electrolysis and anodic-cathodic mixing on the values of the current efficiency. Low values are obtained if the current efficiency is determined before equilibrium has been obtained. The introduction of HCl from the cathode raises the current efficiency for two reasons: the acidity of the solution is increased and the total concentration of Cl^- ions is raised. The values of the current efficiency given here may be considered as minimum values, as any leaks in the apparatus would lower and not raise the values.

TABLE 2.—*Anodic current efficiencies in the counterflow electrolysis of 0.902 N (1:60) solutions of uranyl chloride.*

The graphites were of different commercial grades

Electrode	Current density	Average temperature	Current efficiency	Condition of electrode after use
	amp/cm²	*t° C*	*Percent*	
Platinum	0.025	24.8	97.0	Unchanged.
	.068	22.4	96.8	Do
	.25	22.7	96.9	Do.
	.35	23.6	96.6	Do.
	2.00	24.4	96.7	Do.
	3.33	24.0	96.5	Do.
	4.67	24.2	96.6	Do
Platinum black	0.45	25.9	97.5	Do.
	.64	26.2	96.5	Do.
	.91	25.3	96.6	Black was dispersed.
Palladium	.45	26.9	96.6	Unchanged.
	.64	27.7	96.2	Do.
	.91	28.8	96.2	Darkened.

TABLE 2.—*Anodic current efficiencies in the counterflow electrolysis of 0.902 N (1:60) solutions of uranyl chloride.*—Continued

The graphites were of different commercial grades

Electrode	Current density	Average temperature	Current efficiency	Condition of electrode after use
	amp/cm²	*t° C*	*Percent*	
Palladium black	.45	30.0	96.5	Unchanged.
	.64	30.3	96.4	Black was dispersed.
Iridium	.04	28.3	96.9	Unchanged.
	.08	29.2	96.3	Do.
	.50	26.1	96.5	Do.
Platinum 80%, iridium 20%.	.092	30.3	96.4	Unchanged.
Magnetite	.18	26.0	73.6	Eroded.
	.50	26.5	57.3	Do.
Zirconium carbide	.36	28.2	96.5	Etched.
	.44	28.6	96.0	Do.
	.51	25.7	95.7	Do.
Tungsten carbide	.056	25.1	96.7	Etched.
	.08	25.3	94.5	Do.
	.38	25.0	87.1	Do.
Columbium-tantalum carbide.	.38	26.7	95.5	Slightly etched.
	.53	27.9	95.9	Do.
	.75	26.2	95.1	Do.
Arc carbon	.10	25.2	89.7	Pencilled.
Graphite I	.012	23.9	97.4	Unchanged.
	.017	24.0	96.5	Do.
	.45	22.7	86.5	Do.
	.64	25.2	86.0	Do.
	.90	25.1	85.6	Disintegrated.
Graphite II	.14	30.7	90.0	Unchanged
	.64	28.9	86.7	Do.
	1.25	29.9	85.7	Disintegrated.
Graphite III	0.14	28.8	92.2	Do.
	.64	29.3	84.1	Do.
Graphite IV	.45	29.7	86.6	Do.
Graphite V	.45	27.1	88.8	Do.

TABLE 3.—*Anodic current efficiencies in the counterflow electrolysis of 0.498 N and 0.1 N solutions of uranyl chloride*

0.498 normal

Electrode	Current density	Average temperature	Current efficiency	Condition of electode after use
	amp/cm²	*t° C*	*Percent*	
Platinum	0.015	28.1	87.9	Unchanged.
	.025	28.3	87.5	Do.
	.30	27.7	87.7	Do.
	.50	26.2	87.2	Do.
	2.00	25.9	87.2	Do.
	3.33	27.3	87.2	Do.

0.1007 normal

Platinum	0.01	25.9	57.4	Unchanged.
	.46	26.3	51.3	Do.
	1.36	26.7	45.6	Do.
	1.82	25.2	44.1	Do.
	2.73	27.7	42.3	Do.
Graphite I	0.09	25.6	48.8	Do.
	.18	26.3	45.9	Disintegrated slightly.

TABLE 4.—*Data showing the precision of method for determinations of anodic current efficiencies*

Current density	Average temperature	Current efficiency			
		No. 1	No. 2	No. 3	average
amp/cm²	*C*	*Percent*	*Percent*	*Percent*	*Percent*
Part I: platinum electrodes in 0.902 N solutions of uranyl chloride					
0.025	24.8	97.0	97.1	97.0	97.0
.068	22.4	96.3	97.0	97.1	96.8
.25	22.7	96.8	96.9	.....	96.9
.35	23.6	96.7	96.4	.....	96.6
2.00	24.4	96.7	.....	.....	96.7
3.33	24.0	96.5	96.5	.....	96.5
4.67	24.2	96.6	.....	.....	96.6
Part II: graphite electrodes in 0.902 solutions of uranyl chloride					
0.012	23.9	97.3	97.4	.....	97.4
.017	24.0	96.5	.....	.....	96.5
[a].104	25.2	89.7	.....	.....	89.7
.45	22.7	86.6	86.4	.....	86.5
.64	25.2	86.0	85.9	.....	86.0
.90	25.1	85.5	85.6	.....	85.6

[a] Obtained with arc carbon electrodes in 0.841 N solution of uranyl chloride.

TABLE 5.—*Nonequilibrium values showing the effects of time and anodic-cathodic mixing on anodic current efficiencies*

(Electrodes of platinum and 0.1 N solutions of UO_2Cl_2 were used).

Time of current flow	pH of the overflow	Current density	Current efficiency	Equilibrium value of current efficiency
Effect of the time of electrolysis				
Hours		*Amp/cm²*	*Percent*	*Percent*
2.0	1.67	1.36	8.2	45.6
7.0	1.56	1.82	18.0	44.1
12.0	1.54	1.82	28.2	44.1
24.0	1.52	2.27	39.3	42.3
26.5	1.52	2.73	42.3	42.3
28.0	1.52	.01	57.5	57.4
33.0	1.54	.01	55.0	57.4
36.0	1.52	1.82	44.1	44.1
40.0	1.52	.01	57.5	57.4
42.0	1.52	1.82	43.9	44.1
Effect of anodic-cathodic mixing				
[a]11.5	0.98	1.82	84.7	44.1
26.0	.51	1.82	91.1	44.1
30.0	.58	1.82	90.3	44.1
31.5	1.32	1.82	67.9	44.1
[b]36.0	1.52	1.82	44.1	44.1

[a] This value and all those that follow are the hours of current flow after anodic-cathodic mixing.

[b] No anodic cathodic mixing.

The current efficiency is the same within a few tenths of 1 percent for electrodes of the platinum group and is practically independent of the current density for the most concentrated solutions. For the most dilute solution the current efficiency increases as the current density is decreased. For the other electrode materials the current efficiency is lower. These electrodes for the most part deteriorate with use. Magnetite, in agreement with some observations recorded in the literature [6] deteriorated rapidly forming a cloudy solution. This may explain the abnormally low values of current efficiency obtained with their use. Platinum black and palladium black loosened on use, the black was probably dispersed in the electrolyte.

When the current efficiencies are plotted with respect to the normality of the solutions they approach asymptotically 100 percent as the normality of the solution is increased. This suggests that current efficiencies of 100 percent probably cannot be realized in the electrolysis of aqueous solutions of uranyl chloride at 25° C.

V. Conclusions

The oxidation potentials for the chloride ion and for the water reaction are respectively −1.359 v [7] and −1.229 v [8] at their standard states. In 0.902 *N* solutions of UO_2Cl_2 of pH 1.38, the oxidation potentials of these two oxidation steps are, respectively, −1.379 v and −1.147 v. The activity coefficient of UO_2Cl_2 was taken equal to that of $CaCl_2$ [9] of equivalent concentration. For a partial pressure of oxygen of 0.033 atm. the latter value would be −1.125 v. Thus, even in concentrated chloride solutions, oxygen should be more readily liberated than chlorine. However, because of the bigh oxygen overvoltage, chlorine is evolved.

The percentage yield of chlorine should be greater at those electrodes having the higher oxygen overvoltage and the lower chlorine overvoltage. (The meaning of chlorine overvoltage is obscure. The potential over the reversible potential necessary for chlorine evolution is probably influenced by the presence of oxygen on the electrode surface.) For example, at a current density of 0.1 amp/cm² the oxygen overvoltages for platinum and graphite are about 1.28 v and 1.09 v [10]. These values indicate higher current efficiency for production of chloride at platinum

electrodes. The chlorine overvoltages for platinum and graphite at the same current density are approximately 0.054 v and 0.25 v [10], which likewise indicate higher efficiency at platinum electrodes.

The difference between the overvoltages of oxygen and chlorine is about the same at all current densities for both platinum and graphite (for graphite, the difference decreases slightly with current density), indicating the same efficiency at all current densities. This fact is substantiated by the data for platinum but not for graphite. The latter is probably affected by absorption of evolved gases. If the overvoltage relationships strictly apply, platinum and probably other metals of the platinum group would be the best materials for anodes in the electrolysis of uranyl chloride. However, current efficiencies of 100 percent are not obtained with these electrodes even in concentrated solutions. Hence, simultaneous electrode reactions occur at the anode with the attendant complications arising from changes in acidity and reactions between the electrode products and the electrolyte.

VI. References

[1] A. K. Brewer, S. L. Madorsky and J. W. Westhaver, Science **104,** 2694 (1946).
[2] F. Kohlrausch, Ann. Physik. **62,** 209 (1897).
[3] J. A. Beattie, Int. Crit. Tables, III, 54 (1928).
[4] K. G. Falk, Int. Crit. Tables, VI, 309 (1929); H. S. Harned and E. C. Dreby, J. Am. Chem. Soc. **61,** 3113 (1939).
[5] D. A. MacInnes and E. R. Smith, J. Am. Chem. Soc. **45,** 2246 (1926), **46,** 1398 (1924).
[6] C. L. Mantell, Industrial electrochemistry, p. 107, 118, 336 (McGraw-Hill Book Co., Inc., New York, N. Y., 1940).
[7] D. A. MacInnes, The principles of electrochemistry, p. 199 (Reinhold Publishing Corp., New York, N. Y., 1939).
[8] S. Glasstone, An introduction to electrochemistry, p. 242 (D. VanNostrand Co., Inc., New York, N. Y., 1942).
[9] R. A. Robinson, Trans. Faraday Soc. **36,** 735 (1940).
[10] M. Knobel, Int. Crit. Tables, VI, 340 (1929).

WASHINGTON, April 30, 1946.

718313—47——2

U. S. Department of Commerce
National Bureau of Standards

Research Paper RP1818
Volume 39, August 1947

Part of the Journal of Research of the National Bureau of Standards

Analysis by the Mass Spectrometer of a Liquified Hydrocarbon Mixture Containing C_3-C_5 Paraffins and Olefins[1]

By Vernon H. Dibeler and Fred L. Mohler

A study of two methods for removing small samples from a liquified hydrocarbon mixture of known composition has been made with a mass spectrometer. The first method, that of opening the cylinder valve and allowing the mixture to evaporate slowly into an evacuated reservoir, was shown to give varying compositions depending on the rate of evaporation. The second method employed a low-temperature bath to cool the mixture below the boiling point of all components at atmospheric pressure. A portion of the liquid was then isolated in a pipette and completely expanded into a gas reservoir. Five successive samplings agreed with the composition certified by the Phillips Petroleum Co. within the experimental error.

I. Introduction

During the last 4 years, an increasing number of mass spectrometer laboratories have participated in cooperative test programs designed to evaluate the precision and accuracy of analytical methods for light hydrocarbon analysis. Shepherd [1][2] has recently reported the results of one such cooperative test on a natural gas sample, ASTM D-3-VII-2. The sample batch was carefully prepared in the vapor phase, and all of the cylinders distributed were filled simultaneously from a common manifold. Other test programs, however, have required analysis of liquefied hydrocarbon mixtures in which the relatively minute sample used by the mass spectrometer was removed from the liquid phase, usually by evaporation. Some of the variations in reported composition of the liquefied hydrocarbon mixture may be due to real differences in the composition of the separate samples sent to different laboratories. More likely, however, is a change in composition caused by inadequate precautions taken to remove a representative sample from the liquefied contents of the cylinder. To minimize the possibility of the former, a large batch of the test sample was usually divided into a number of portions and each portion put into a cylinder using various means to maintain identical composition for each sample. Assuming such precautions to be effective, however, it should be noted that at least one case has been reported [3] in which the composition of a liquefied hydrocarbon mixture changed over a period of time due to distillation through a slowly leaking valve.

It has long been known that it is very difficult to remove a representative sample from the liquid phase of a two or more component system boiling below room temperature at atmospheric pressure. Shepherd [2] has listed the steps necessary to do this as, (1) the liquid phase is made homogeneous, (2) a portion of the liquid phase is isolated from the bulk of the liquid without change in composition (i. e., without boiling), (3) the isolated portion is completely evaporated into a suitable container again without change in composition, and (4) the vapor phase is made homogeneous.

This paper reports a series of mass spectrometric analyses made on Phillips Hydrocarbon Mixture 21, containing C_3–C_5 paraffins and olefins. The boiling range was approximately −48° to +37° C; the freezing range was approximately −188° to −105° C. The samples for analysis were withdrawn from the cylinder by two methods. First, the valve of the inverted cylinder was cautiously opened to admit a quantity of gas into an evacuated reservoir; and second,

[1] This work was financed in part by funds made available by the Reconstruction Finance Corporation, Office of Rubber Reserve.

[2] Figures in brackets indicate the literature references at the end of this paper.

[3] Phillips Hydrocarbon Mixture 6 as received by the Gas Chemistry Section, National Bureau of Standards.

a small portion of the liquid phase was isolated from the bulk of the liquid without appreciable change in composition and completely evaporated into the reservoir. For samples taken by the first method, the variation in composition was studied as a function of the flow-rate. The apparent composition of samples taken by both methods were compared with each other and with the composition certified by the Phillips Petroleum Co.

II. Experimental Procedure

The hydrocarbon analyses were made with a Consolidated mass spectrometer [3]. The hydrocarbon mixture was blended by the Phillips Petroleum Co. as mixture No. 21 with the composition reported as accurate to ± 0.05 percent. It was received in an ICC specification steel cylinder fitted with a standard liquefied petroleum gas valve. A number of samples for analysis were removed from the liquid phase by each of the two methods described below. The data obtained by the mass spectrometer were evaluated with a Consolidated electrical computer [4] using procedures recommended by the manufacturer.

The procedures for the two methods of sampling are outlined below.

Method I. The cylinder, with a needle valve and inner member of a standard taper attached, was supported in an inverted position. The air in the needle valve connection was carefully flushed out and the cylinder attached to a 5-liter glass reservoir (*A* in fig. 1) by the outer standard taper, *C*. All volumes and connections up to the needle valve were evacuated to about 10^{-4} mm. At this point, the reservoir was isolated from the rest of the system by closing the metal sylphon valve, *D*. The inner surfaces of the reservoir and connections were then "conditioned" with the hydrocarbon mixture by cautiously opening the needle valve until a pressure of several centimeters was indicated on the manometer, *B*. The needle valve was then closed and the reservoir and connections evacuated through *D* to a pressure of less than 0.1 mm, as shown on *B*. The flushing was repeated twice at approximately the same rate. A sample for analysis was then removed from the cylinder at approximately the same rate as the flushing by opening the needle valve until a desired pressure was read on the manometer, *B*. The rate of flow obtained for any opening of the needle valve was calculated from the time required to introduce sufficient gas to raise the pressure in the reservoir to 15 mm. For the slowest rate measured, this required about 100 seconds, while the most rapid sampling attempted required only 15 seconds. The contents of the reservoir were mixed by convection, and a 5-ml portion isolated in the volume, *G*. This portion was then condensed at liquid air temperature into one of the lengths of 3-mm tubing on manifold *H*, and sealed off. Care was taken to adjust volumes and pressures so that the contents of the 3-mm tubing could be released directly into the inlet reservoirs of the mass spectrometer without further subdivision.

Method II. A small liquid pipette was constructed by soldering two needle valves to a sufficient length of ½-in. copper tubing to give a 3-ml volume between the valve seats. One end of the pipette was provided with a standard taper to connect to the gas reservoir (fig. 1); the other end

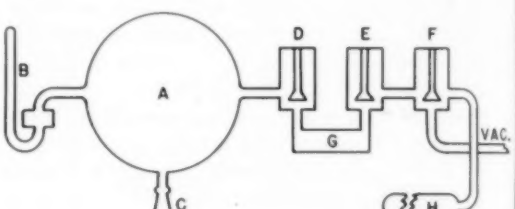

FIGURE 1.—*Schematic drawing of gas phase sampling and bottling apparatus used for methods I and II.*

was connected to the hydrocarbon cylinder by a suitable fitting. The air was flushed out of the pipette and with valve, *M*, closed, the unit was partially submerged in a low temperature bath (−78° C) as shown in figure 2. The glass tube, *L*, was added before submerging to prevent contamination and to provide a means of flushing a known amount of liquid through the pipette. After 5 minutes of cooling, the unit was removed from the bath, thoroughly shaken and replaced. After this procedure was twice repeated, liquid hydrocarbon was flushed through the pipette by cautiously opening *M* and allowing the liquid

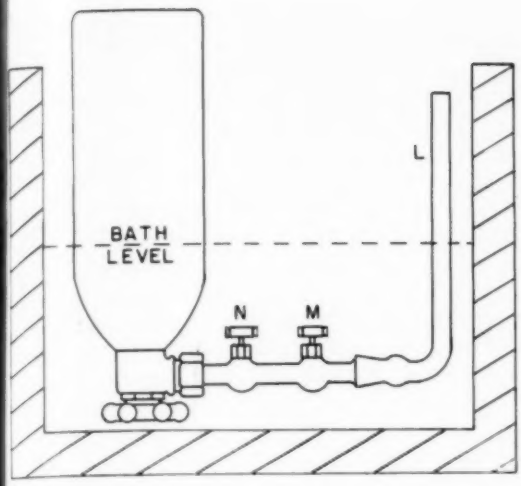

FIGURE 2.—*Hydrocarbon cylinder and liquid pipette as supported in the low temperature bath for use in method II.*

to slowly rise in the vertical glasss tube, *L*.[4] When the level in *L* indicated a complete change of liquid in the pipette, *M* and *N* were closed and the unit connected to *C* (fig. 1). Thereafter it was removed from the bath, allowed to come to room temperature and the entire contents evaporated into the gas reservoir. The gas phase was then thermally mixed and sampled as described in method I.

The calibrating gases were Phillips Research Grade Hycrocarbons with the exception of *cis*-2-butene, 1-pentene and *trans*-2-pentene. The *cis*-2-butene was a Mellon-Koppers-Hinckley sample previously described by one of the authors [5]. The 1-pentene and *trans*-2-pentene were standard samples numbers 281–5S and 283–5S, respectively, available at the National Bureau of Standards.

III. Discussion of Results

The analysis of isomers in the mass spectrometer is, in general, inferior to the analysis of substances differing in molecular weight. The discrimination between butenes is particularly difficult. The following pages give complete analyses and also data for total butenes, butanes, pentenes and pentanes. Figures for the totals are usually more accurate than for separate isomers, and are in some respects a better test of the sampling techniques.

Table 1 shows the composition of the hydrocarbon samples as a function of the sampling rate when removed from the cylinder by method I. Columns 2 to 7 inclusive are given in the order in which the samples were taken and at the flow-rate in milliliters per second indicated at the head of each column. Column 9 lists the composition reported by Phillips as accurate to ±0.05 percent. The reproducibility of composition for the same flow-rate, as indicated by the three analyses sampled at two milliliters per second, is interesting in that it shows reproducibility to be a poor criterion of a representative sample when the sample is taken in this manner. Further evidence of this fact is given in table 2, which shows the results of six analyses made on the same hydrocarbon mixture as part of a Rubber Reserve cooperative program. In this case, the cylinder was directly attached to the mass spectrometer inlet, and vapor metered into the reservoirs. As they are obviously not representative samples, the reproducibility is unusual; although an experienced analyst will often sample at nearly the same rate several times in a row. A relatively slow rate is required to guard against breakage and observations on similar samples show the usual sampling rate in this laboratory to be about two milliliters per second.

TABLE 1.—*Mole percent composition of samples obtained by vaporizing a stream of liquid*

Component	Sample flow rate (ml/sec)[a] and mole percent							Synthetic composition
	2	5	1	2	2	3	7	
Propene	5.5	6.6	5.2	5.4	5.5	6.0	6.8	7.00
Propane	10.3	10.4	10.0	10.3	10.2	10.5	10.8	10.55
1-Butene	7.1	8.7	5.8	6.1	6.8	7.2	6.7	8.28
2-Butene	9.2	9.9	7.7	8.9	8.1	9.7	11.9	6.24
i-Butene	4.5	2.2	7.1	5.8	5.8	4.0	2.0	6.10
n-Butane	30.0	30.2	29.9	30.1	30.0	30.3	29.9	29.88
i-Butane	14.1	13.0	14.7	14.0	14.3	12.9	13.1	13.25
1-Pentene	2.4	2.5	2.2	2.4	2.2	2.5	2.1	1.65
2-Pentene	1.3	1.1	1.6	1.3	1.5	1.1	1.4	1.69
n-Pentane	8.9	8.8	9.1	9.1	9.1	8.9	8.7	8.88
i-Pentane	6.7	6.7	6.7	6.6	6.4	6.8	6.6	6.48
Total Butenes	20.8	20.7	20.6	20.8	20.7	20.9	20.6	20.62
Total Butanes	44.1	43.1	44.6	44.1	44.3	43.2	43.0	43.13
Total Pentenes	3.7	3.6	3.8	3.7	3.7	3.6	3.5	3.34
Total Pentanes	15.6	15.5	15.8	15.7	15.5	15.7	15.3	15.36

[a] These measurements are tabulated in the order in which they were made

[4] On one or two occasions it was necessary to direct a stream of warm air on the upper end of the cylinder to initiate the flow of liquid.

TABLE 2.—*Mole percent composition of six samples evaporated directly into mass spectrometer reservoir*

Component	Sample Number and Mole Percent						Mean	Synthetic composition
	1	2	3	4	5	6		
Propene	5.2	5.2	5.5	5.5	5.5	6.0	5.5±0.2	7.09
Propane	10.3	10.3	10.3	10.3	10.4	10.5	10.4± .1	10.55
1-Butene	6.8	6.1	5.5	7.1	6.6	8.7	6.8± .7	8.28
2-Butene	8.1	8.9	9.1	9.2	8.8	9.9	9.0± .4	6.24
i-Butene	5.8	5.8	6.0	4.5	5.4	2.3	5.0±1.0	6.10
n-Butane	29.9	30.0	29.9	30.0	30.2	30.2	30.0±0.1	29.88
i-Butane	14.3	14.0	14.2	14.1	13.7	13.0	13.9± .4	13.25
Total pentenes	3.8	3.8	3.7	3.7	3.7	3.8	3.7± .1	3.34
n-Pentane	9.1	9.2	9.0	8.9	9.0	8.8	9.0± .1	8.88
i-Pentane	6.7	6.7	6.8	6.7	6.7	6.8	6.7± .1	6.48
Total Butenes	20.7	20.8	20.6	20.8	20.8	20.9	20.8± .1	20.62
Total Butanes	44.2	44.0	44.1	44.1	43.9	43.2	43.9± .2	43.13
Total Pentanes	15.8	15.9	15.8	15.6	15.7	15.6	15.7± .1	15.36

The variation of composition as a function of the rate of sampling is shown graphically in figure 3. The ordinate of a point plotted for a component represents the percent of the known composition actually found in the sample taken at the flow-rate indicated by the abscissa. For example, the amount of propene determined in a sample taken at a rate

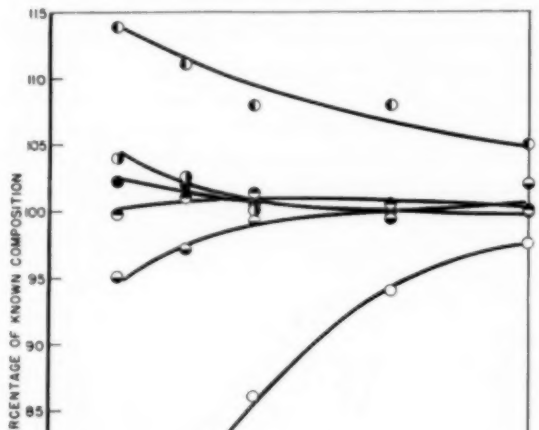

FIGURE 3.—*Percentage of known composition of the components plotted as a function of the sample flow-rate in method I.*

○, propene; ◒, propane; ◓, butenes; ◑, butanes; ◐, pentenes; ●, pentanes.

of 1 ml per second was 5.2 percent. This represents only 74.3 percent of the reported concentration of propene in the original mixture. In the same sample, propane was analysed as 10.0 percent, or 95.7 percent of the known concentration. The other components are similarly plotted. Total butenes, butanes, pentenes, and pentanes are plotted because of the uncertainty of distribution between the isomers as mentioned above. The deviation from known composition is less marked with increased sampling rate. This may be the result of cooling at the valve seat, in which case, the lower boiling components pass through the valve before completely evaporating.

In 1920, A. K. Dunbar of the Harvard Cryogenic Laboratory studied the sampling of the system, liquid nitrogen+oxygen, under various conditions and at different rates of flow. His work, described in a series of reports to the U. S. Bureau of Mines, disclosed an isobaric separation yielding high nitrogen. This is in the expected direction, and the effect observed in the present work reverses this expectancy. In the effort to avoid possible misunderstanding in comparing cross-check analyses, Shepherd called attention to Dunbar's work in a 1944 report to Rubber Reserve, and at the same time added an observation he had made in 1920 with respect to the operation of a helium still. A still plate containing approximately equal parts of nitrogen and methane at 300 lb/in.^{2} delivered essentially nitrogen from a needle valve located outside of the still lagging, whereas much nearer the proper mixture was delivered from a needle valve whose seat was located within the still plate itself. This experiment magnified the effect to be expected upon sampling systems like the C_{3+4+5} mixtures under pressure in cylinders delivered for Rubber Reserve cross-check analyses. As stated above, these effects are in the opposite sense to the effects shown in figure 3. An effect in the direction indicated by figure 3 could arise from an accumulation of unvaporized higher boiling components resulting from the process of conditioning the large reservoir in method I or the mass spectrometer inlet manifold in table 2. In the authors' opinion, the effect could also arise from depletion of the liquid near the needle valve with respect to the more volatile components, due to bubbles rich in these components moving under gravity in a direction opposite to the sample stream, except

when the latter flow-rate is high. The former phenomenon has been observed in distillation apparatus while the latter is hypothetical. The important point, however, is that sampling by method I can lead to erroneous results.

Table 3 gives the composition of six samples removed from the cylinder by method II. Sample six was taken immediately after a large amount of liquid hydrocarbon was lost from the cylinder and is not included in the average values listed in column 8. For this sample, the space above the liquid in the cylinder was probably large enough to allow an appreciable change in the composition of the liquid due to a greater evaporation of the lower boiling components. Total isomers of each component are tabulated for comparison with table 1. The variation in distribution among the isomers is considerably less than in table 1 and slightly less than usually encountered in such a mixture as shown in table 2. Since the 2-butene calibration was made using the *cis*-2-butene isomer, some small error may be expected if the *trans* isomer is present in the mixture. The variation in the butenes, however, is less than that expected if ± 0.5 percent pattern variation is assumed. Although the *trans*-2-pentene isomer was used to calibrate for 2-pentene, negligible error is expected since the *cis*- and *trans*-2-pentene patterns are more nearly alike than the patterns of the 2-butene isomers.

The Consolidated electrical computer was used to solve the 11 simultaneous equations. The most arduous task was the proper preparation of the matrix to assure rapid convergence in the computer. This preparation was aided by the use of 132 small wooden blocks arranged 11 by 12 in a tray and constructed in a manner that allowed any two rows or columns to be picked up and their positions exchanged. This was similar to the more elaborate checkerboard used for the same purpose in the Gas Chemistry Section of the Bureau. The coefficients and constant terms were then written on labels glued to the blocks. Several arrangements of the matrix were tried. None were more suitable than that suggested by Consolidated, except in one set of analyses in which carbon dioxide was accidentally added to the mixture. The time required for each solution was about 45 minutes. This includes time for setting in or checking the coefficients already in the computer prorated for all analyses. At first some difficulty was experienced with variable contact resistance between the helipots representing the coefficients and the contactor bar resulting in no solution or spurious results. This diminished with continued use, and under present conditions the data obtained for any of the above reported samples solved on successive trials give checks to ± 0.2 percent of the value. This is much better than the reproducibility of the mass spectrometer data obtained for this mixture.

TABLE 3.—*Analyses of samples removed in the liquid phase*

Component	Sample number and mole percent						Mean 1 to 5	Synthetic composition
	1	2	3	4	5	[a]6		
Propene	7.1	7.0	7.2	6.7	7.1	6.3	7.02±0.14	7.00
Propane	10.7	10.5	10.6	10.7	10.6	10.5	10.62± .06	10.55
1-Butene	7.6	8.8	8.4	8.0	8.0	8.3	8.12± .34	8.28
2-Butene	6.3	6.0	6.1	5.9	5.8	6.4	6.02± .14	6.24
i-Butene	6.5	5.8	5.9	6.5	6.7	5.8	6.28± .34	6.10
n-Butane	30.2	30.2	29.4	29.4	29.7	29.3	29.78± .22	29.88
i-Butane	13.1	13.1	13.6	14.0	13.5	14.3	13.46± .29	13.25
1-Pentene	1.6	1.6	1.8	1.6	1.6	1.6	1.64± .06	1.65
2-Pentene	1.8	1.8	1.7	1.8	1.8	1.8	1.78± .03	1.69
n-Pentane	8.6	8.7	8.8	8.6	8.5	8.4	8.64± .09	8.88
i-Pentane	6.5	6.5	6.5	6.8	6.7	7.3	6.60± .12	6.48
Total butenes	20.4	20.6	20.4	20.4	20.5	20.5	20.46± .07	20.62
Total butanes	43.3	43.3	43.0	43.4	43.2	43.6	43.24± .11	43.13
Total pentenes	3.4	3.4	3.5	3.4	3.4	3.4	3.42± .03	3.34
Total pentanes	15.1	15.2	15.3	15.4	15.2	15.7	15.24± .09	15.36

[a]Sample 6 was drawn from a nearly empty cylinder.

IV. Conclusions

The foregoing experiments indicate that a common technic of sampling volatile liquid mixtures, namely, permitting a slow stream of liquid to evaporate into an evacuated volume, can lead to large systematic errors in the analysis. In the Phillips hydrocarbon mixture 21, samples introduced into previously flushed reservoirs at slow rates were deficient in propene and rich in butanes and pentenes. Other components showed smaller effects. The error was reduced if the sampling rate was increased. The error was minimized, however, by withdrawing a small liquid sample from the cylinder without change in composition at the point of withdrawal. This can be done within the limits of error of the present mass spectrometer by lowering the temperature of the cylinder and contents in the vicinity of the valves to a temperature sufficiently below the boiling point of all components at atmospheric pressure and a sample removed as described above.

The analysis of a volatile mixture on the basis of a liquid sample involves the assumption that a negligible amount of the mixture is in the gas phase. As the ratio of liquid to gas density at atmospheric pressure is 200–300 to 1, the gas phase clearly can be neglected if the liquid nearly fills the container. If it is nearly empty, the liquid is no longer representative of the mixture within the precision of the analyses. It has been noted before that sample 6 of table 3 is measurably depleted in propene for this reason. Samples 1 to 5 of table 3 obtained from a nearly full container show in general a mean composition agreeing with the synthetic composition within the range of experimental uncertainty. For propene, propane, total butenes, butanes, pentenes, and pentanes, this uncertainty is of the order of 0.1 percent of the total amount. The discrimination between isomers is considerably less accurate than this.

Recent modifications of the Consolidated mass spectrometer that were not used in this work may reduce the experimental error somewhat. They will, however, emphasize the importance of improved sampling procedure.

The authors wish to acknowledge the value of many helpful discussions with Martin Shepherd on this subject. The mass spectrometer was operated by Robert M. Reese, and computations were made by Dorothy Thompson and Laura Williamson.

V. References

[1] Martin Shepherd, J. Research NBS **38,** 491 (1947) RP1789.

[2] Martin Shepherd, National Bureau of Standards. Publication pending.

[3] H. W. Washburn, H. F. Wiley, S. Rock and C. E. Berry Ind. Eng. Chem. Anal. Ed. **17,** 74 (1945).

[4] C. E. Berry, D. E. Wilcox, S Rock, and H. W. Washburn, J. Appl. Phys. **17,** 262 (1946).

[5] V. H. Dibeler, J. Research NBS **38,** 329 (1947) RP1775.

Washington, April 15, 1947.

U. S. Department of Commerce
National Bureau of Standards

Research Paper RP1819
Volume 39, August 1947

Part of the Journal of Research of the National Bureau of Standards

An Indentation Method for Measuring Wear

By Samuel A. McKee

This paper describes a method for accurately measuring the wear that takes place on the bearing surfaces of machinery. The method consists of making minute indentations in the wearing surface by means of a specially shaped diamond point. As material is worn from the surface, the dimensions of the marks change with the amount of material removed. Measurements of the dimensions of these marks before and after wear provide a means for determining the amount of wear that has taken place.

Apparatus is described for using this method for the measurement of wear occurring in the cylinders of aircraft engines. The results of tests with engines in operation indicate that the method is practicable. Curves are also given showing typical wear data obtained in engine cylinders.

The chief advantages of the method over the usual methods are (1) greater accuracy, (2) a precise indication as to where wear occurs, and (3) the measurements are not affected by growth, shrinkage or distortion of the machine element under test.

I. Introduction

One of the major difficulties in the determination of the wear of machinery has been the lack of a convenient method for measuring directly the amount of material removed. Among the methods that have been commonly used are the weighing of the parts before and after wear, the measurement of the dimensions of the parts before and after wear, and the determination of the amount of worn material found in the lubricant after operation.

In some cases, more especially with laboratory apparatus, the parts are of such size and shape that the wear may be determined with reasonable accuracy by weighing or by measuring the dimensions. In the normal operation of many machines, however, the amount of material worn off in a reasonable time is so small compared to the size of the part as to make it impracticable to determine the wear by loss in weight. The method of measuring changes in dimensions requires sensitive apparatus and painstaking technic to obtain the accuracy required. Even under ideal conditions both of these methods have some serious limitations. The weighing method gives a value for the total wear but does not indicate where the wear occurred. The method of measuring the changes in the dimensions of the part has this same limitation to a lesser degree in cases where wear occurs upon both surfaces that determine a given dimension. This method also does not differentiate between actual wear and other changes that may occur such as growth, shrinkage, or distortion of the part. The method of determining the amount of worn material in the lubricant presents a number of difficulties and usually is used only as a qualitative indication in conjunction with other data.

These limitations indicate the desirability of developing a method or methods of measuring wear that are independent of the size or mass of the part. The idea of the use of such a method is not new. For years engineers have used the appearance of the tool marks on a part as an approximate indication of the amount of wear. This practice suggested an investigation to determine the practicability of a method of measuring the amount of material worn off. This was done by applying to the working surfaces marks of such a shape that a relatively small amount of wear would make a definite change in one or more readily measurable dimensions of the marks and

hence provide a measurable indication of wear at the points where the marks are made.

The problem of particular interest in this investigation was the study of wear in radial aircraft engines, especially in the cylinders where the conditions are such that permanent distortion might occur during operation that could nullify, from the standpoint of measuring wear, the significance of even the most careful measurement. The apparatus therefore was designed primarily to locate and measure marks on the cylinder walls of a radial aircraft engine, although provision was also made for measuring the pistons.

II. Method and Apparatus

The choice of the particular type of mark used in this investigation was influenced by the fact that at the National Bureau of Standards there was already under development an indentation method for measuring the hardness of materials that utilized a mark that appeared to be readily adaptable for the measurement of wear. This hardness apparatus is known as the Knoop Indenter.[1] The indentation is made by pressing into the surface the apex of a four-sided diamond pyramid having a rhombus-shaped base. The diamond used in these wear tests is of the same general shape as the Knoop diamond but differs in essential dimensions. Greatly enlarged views of a typical indentation are shown in figure 1. The views on the left from top to bottom are the plan, longitudinal section, and transverse section respectively of a mark before wear has occurred, while those on the right are the respective views of the same mark after material has been removed from the surface. From this figure it will be noted that the shape of the mark remains the same, but the length decreases in proportion to the thickness of material removed. With the diamond used in these tests the ratio of depth of mark to length of long axis is about 1 to 35, that is, a mark about 0.001 in. deep has a long axis of about 0.035 in.

Special apparatus was developed for making and measuring these marks. A cylinder or piston to be tested is placed in a special fixture, and marks at any desired position on the surface are applied to a predetermined depth by means of the diamond point, which is forced by mechanical

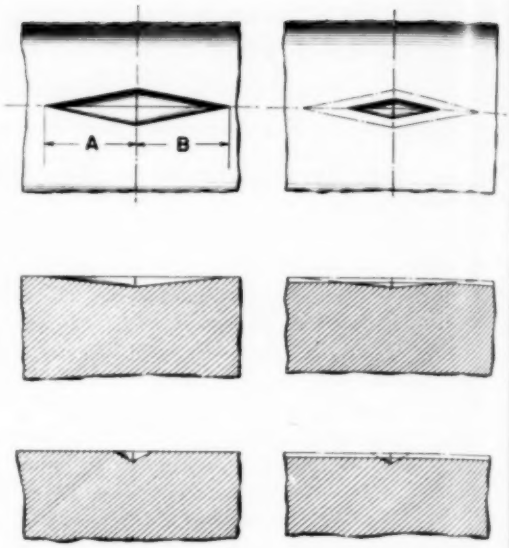

FIGURE 1.—*Enlarged views of typical indentation.*

pressure through suitable cams and levers into the surface of the part. A photograph of the apparatus for indenting the cylinders is shown in figure 2 and a drawing of this apparatus in figure 3.

FIGURE 2.—*Apparatus for indenting cylinders.*

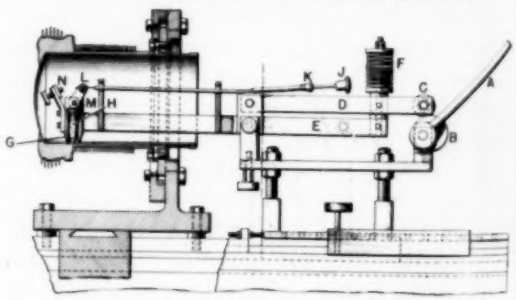

FIGURE 3.—*Drawing of apparatus for indenting cylinders.*

[1] Frederick Knoop, Chauncy G. Peters, and Walter B. Emerson, J. Research NBS **23**, 39 (1939) RP1220.

In making an indentation, the cylinder is mounted in the fixture as shown in figure 3. The cam lever, *A*, is moved by one hand of the operator to rotate the cam, *B*, in engagement with the roller, *C*, and raise lever, *D*. The upward movement of *D* is communicated to lever, *E*, through the spring assembly, *F*. This depresses the indentation head, *G*, until it is clamped solidly against the surface of the cylinder by the force of spring, *F*. The indentation pin, *H*, carrying the diamond indentor is then depressed by the other hand of the operator by pushing the plunger, *J*, into its handgrip, *K*, thus moving the link, *L*, and actuating the indentation cam, *M*, on the indentation head. The cam contacting with the head of the indentation pin forces it downward and impresses the diamond indentor into the surface of the cylinder, the stop, *N*, regulating the depth of the mark. On removal of both hands the indentation head and pin return to their original position. The apparatus is arranged for the use of both hands in order to prevent the operator moving the cylinder relative to the indenter until the diamond is in a safe position.

The viewing and measuring apparatus consists of a conventional microscope and eye piece scale except that the tube is lengthened and two right-angle prisms inserted to permit use as a periscope to view the inside of the cylinders. A photograph of this apparatus as used in measuringa mark on a piston is shown in figure 4.

A particular advantage of the use of this method and apparatus is that it provides an indication of wear only, while the usual measurements of changes in diameters of the pistons and cylinders do not differentiate between wear and such distortion as may occur during a test. A further advantage is that it indicates the wear at a particular point on the surface, whereas the measurements of diameter involve changes at two points, and usually there is no practical method of determining how much of the wear occurred at either one. Also, the method does not require the careful technic necessary to measure diameters with corresponding accuracy. Temperature variations do not materially affect the accuracy with the indentation method, hence it is not necessary to bring the cylinder to a standard temperature before making the measurements. This results in a saving in time. In this connection, the apparatus is provided with locating pins, and is so arranged that a mark made at given pin settings will fall within the field of vision of the periscope when using the same settings. This eliminates loss of time in searching for the marks that are too small to be readily discernable to the eye.

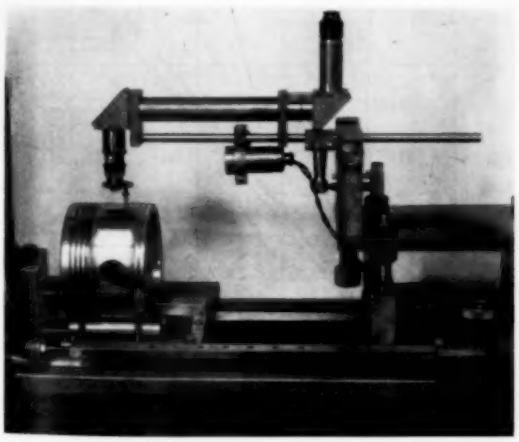

FIGURE 4.—*Apparatus for viewing and measuring indentations.*

III. Preliminary Experiments and Calibration

Preliminary experiments were made to determine whether the marks would retain their shape sufficiently well to provide reasonable accuracy of measurement. A study of grinding and lapping operations using flat blocks suitably indented indicated that there was probably greater likelihood of the mark retaining its shape when the long axis of the base is perpendicular to the line of motion of the rubbing surfaces. With the lapping operations it was found that when the motion was parallel to the long axis the scratches tended to obscure the points of the mark. Subsequent trial runs in engines indicated that marks perpendicular to the axis of the cylinder were in general satisfactory for the purpose.

Accurate measurements were made of the contour of the diamond in order to determine the ratio of depth to the long axis of an indentation. It was felt, however, that greater accuracy could be obtained by direct calibration of typical indentations made in various materials. As the

indentations are made by pressing the diamond point into the metal it would be expected that the marks would be shallower than the diamond point because of the elastic recovery of some of the metal after the stress was removed. These calibrations were obtained by comparing the changes in lengths of indentations placed on flat blocks of cylinder and piston materials with direct measurements of change in thickness occurring when material is lapped from the surfaces.

The results of these calibrations are given in figure 5 where the wear (average depth of material lapped from the surface) is plotted against the average change in length for a number of marks on a given block. The ratio of change in length

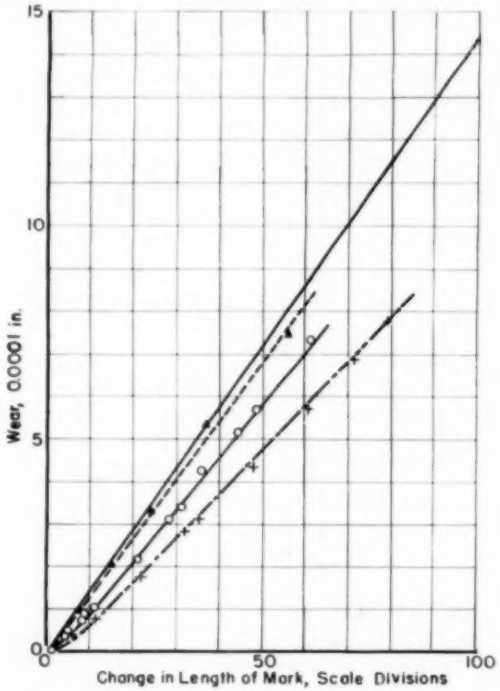

FIGURE 5.—*Indentation calibration curves for various materials.*

——— diamond indenter; ▲— — —, aluminum alloy (piston); ○ ———, steel (cylinder); +——— — ———, nitrided steel (cylinder).

to change in depth based on measurements of the contour of the diamond is also shown in figure 5. Comparison of the curves in this figure indicates that the deviations of the marks from the dimensions of the diamond follow the order of hardness. The curve for the relatively soft aluminum alloy piston material is the closest to the curve for the diamond, while the greatest deviation is shown for the very hard nitrided steel.

The action of impressing the marks in the surface of the metal raises a burr around the mark. The shape of the diamond is such, however, that the major portion of the burr is formed on the sides of the mark. There is no apparent burr visible to the eye at the ends of the marks, but the presence of a very slight raising of the surface at the ends may account for the slight deviations from a straight line shown by the calibration curves. In the course of the investigation it was found that most of the burr could be easily removed by rubbing lightly with fine polishing paper. For use with the cylinders, a sheet-metal guard similar to the usual erasing shield but of larger dimensions was found convenient. The holes in this guard were so arranged that the polishing paper could be rubbed with one finger over a small area at each mark on the cylinder wall.

As the marks are placed with their long axes perpendicular to the axis of the cylinder, the relation between the change in depth of mark to change in length of long axis is affected by the curvature of the cylinder. While this effect is relatively small for the particular cylinders used, suitable corrections for curvature provide greater accuracy in determining wear. The calibration curve corrected for curvature for the chrome-molybdenum steel cylinders used in most of the engine tests is shown in figure 6. The corrections for curvature

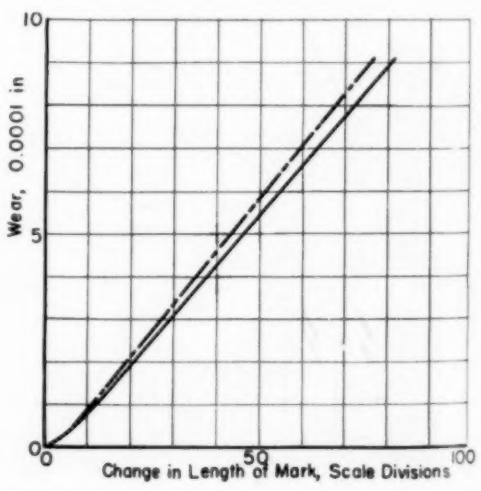

FIGURE 6.—*Corrections for curvature of the cylinder.* ——— — ———, *flat block;* ———, *correction for curvature.*

are based upon a mark having a length of 0.032 in. and upon a cylinder diameter of 5⅜ in., these values being representative of most test conditions.

A study was also made of the possibility of error due to the base of the diamond indenter not being parallel to the surface when the indentation is made. This would result in an unsymmetrical mark. Computations indicated that if the diamond-shaped mark was symmetrical to within a ratio not less than 41 to 50 along its major axis (ratio of dimension "*A*" to "*B*" in fig. 1), the error would be not greater than 1 percent (approximately 0.00001 in.). It was found that the apparatus could be adjusted to produce a symmetrical mark, and that other marks either in the same cylinder or in other cylinders of the same nominal size could be made well within the limits of symmetry without further adjustment. Accordingly, no corrections for lack of symmetry were necessary.

IV. Performance of Marks in Service

One of the important considerations in this investigation was the question as to whether the marks would retain their shape during the operation of the engine. Results of a number of engine tests have shown that marks made in the cylinders of radial aircraft engines retain their shape sufficiently to provide reasonably accurate wear measurements. Photographs of marks in cylinders that were taken after the engines had been operated are shown in figures 7 and 8. The views in figure 7 are typical of most of the marks observed. In a few cases the marks were distorted to the extent shown by the views in figure 8. The right-hand view in this figure is unusual in that the metal has flowed over part of the mark. Experience has shown that most of the poor marks occur when they have been worn to about one quarter of their original length or less, hence greater accuracy may be obtained by so regulating size of mark and length of test to avoid this condition.

The scales shown in the views in figures 7 and 8 represent an actual length of 1 mm (0.0394 in.), and the marks were originally about 0.9 mm. When observed in the viewing apparatus the scale is about 2½ in. long. With the diamond used and with the chrome-molybdenum steel cylinders the total length of the scale represents about 0.0012 in. in depth, hence one of the small-scale divisions

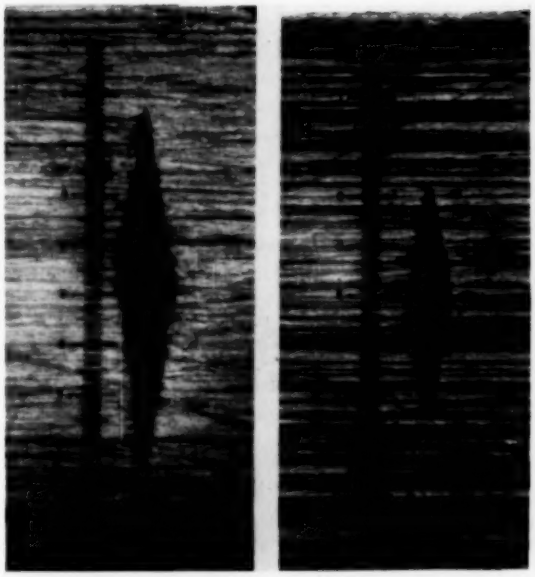

FIGURE 7.—*Typical marks in cylinders after operation.*

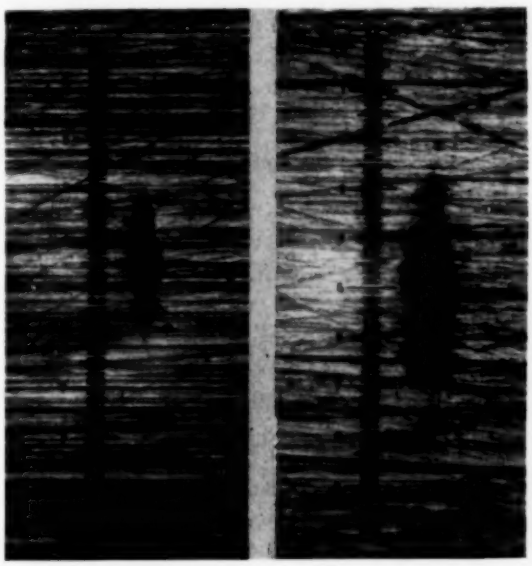

FIGURE 8.—*Cylinder marks that were distorted by operation.*

is equivalent to slightly more than 0.00001 in. of wear. This gives an idea as to the order of sensitivity of the method.

The accuracy of the wear measurements, of course, depends upon the condition of the mark. With new marks the points are sharp and the

lengths can be accurately determined. After the engine has been operated however, as is seen in the figures, the marks are somewhat blunted and it is necessary to estimate the position of the point. It is estimated that under normal conditions the wear can be determined with an over-all accuracy of ± 0.00004 in. Under favorable conditions this figure can be reduced to ± 0.00002 in. This estimate applies to the determinations of cylinder wear. Operating experience with marks in the pistons indicates that with the softer aluminum alloy the marks have a much greater tendency to distort, and the results are not especially satisfactory. Photographs of typical marks in pistons after operation are given in figure 9. Another

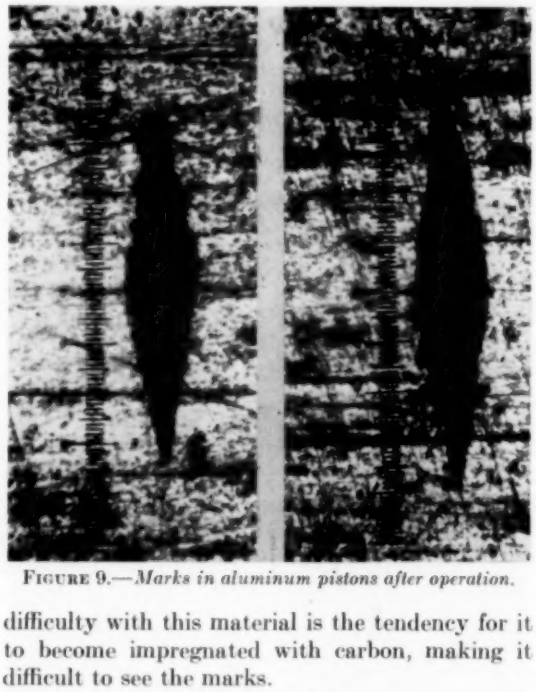

FIGURE 9.—*Marks in aluminum pistons after operation.*

difficulty with this material is the tendency for it to become impregnated with carbon, making it difficult to see the marks.

A second consideration of importance in this investigation was whether the presence of the marks materially affected the lubrication in the cylinder. Apparently they had little effect. This is illustrated by the views in figures 7 and 8 where it is seen that the surface scratches and ridges passing through a mark are not materially different from those beyond the ends of the mark. In this connection, the viewing apparatus provides a convenient means for the microscopic examination of the surface conditions in the cylinders.

V. Typical Wear Patterns in Engine Cylinders

Most of the engine tests for the study of the performance of the marks in service were made with radial aircraft engines having chrome-molybdenum steel cylinder barrels $5\frac{3}{16}$ in. in diameter. In these tests 24 marks were made in each cylinder, 6 spaced 60 degrees apart at each of 4 levels. These levels were approximately 2, 4, 6 and 8 in. respectively from the open-skirt end of the cylinder. The upper row of marks was near the top of the ring travel and was in contact with the top ring only while the lower row was contacted by the oil ring only.

Typical cylinder-wear patterns obtained in these tests are shown in figures 10, 11 and 12. In these figures the wear at each of the four levels is plotted as ordinates and the angular position of the marks as abscissas. The angular locations are taken in a clockwise direction when looking into the open end of the cylinder. Zero (0

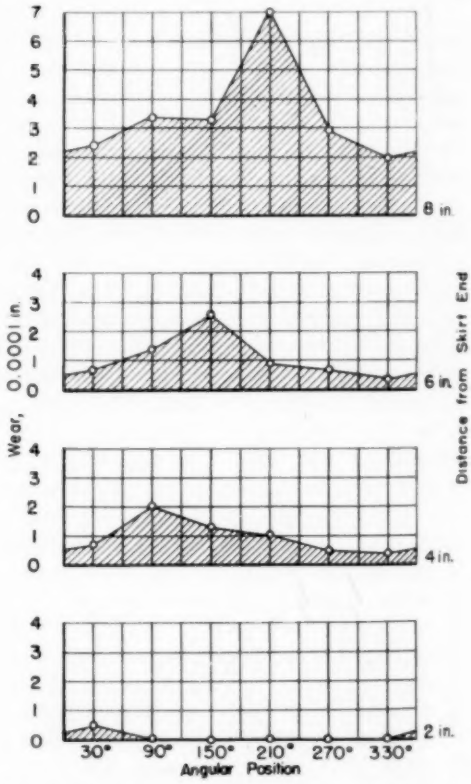

FIGURE 10.—*Wear in cylinder of radial aircraft engine.*

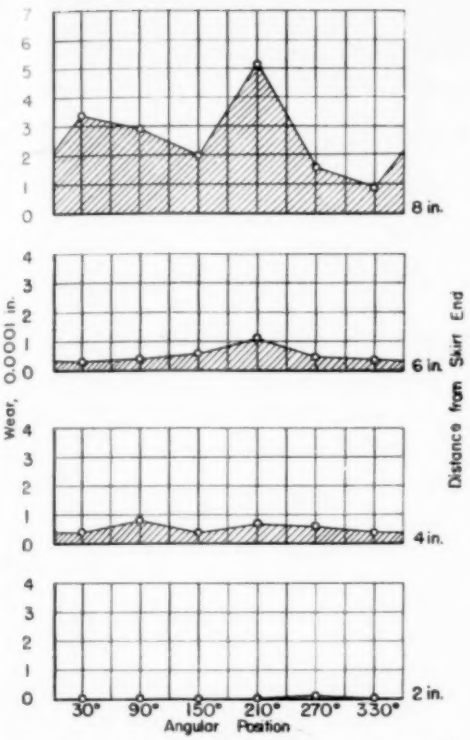

FIGURE 11.—*Wear in cylinder of radial aircraft engine.*

degrees is at the center line of the spark-plug hole located between the rocker-arm cages.

These figures are of interest in that they indicate an unsymmetrical wear with respect to the axis of the cylinder that would be impossible to determine with the usual measurements of diameter.

VI. Conclusion

The data given in this paper indicate that the indentation method is practicable for the measurement of wear in radial aircraft engine cylinders. It is apparent that the method is also applicable for use on other machine elements, gages, dies, and other wearing surfaces where the material is of such a nature that the marks will retain their shape in service.

The method is covered by U. S. Patent No. 2,233,403, granted to H. C. Dickinson and S. A. McKee on March 4, 1941, and assigned by them to the United States Government. The American Instrument Company, Silver Spring, Md. was licensed to manufacture the instrument by the

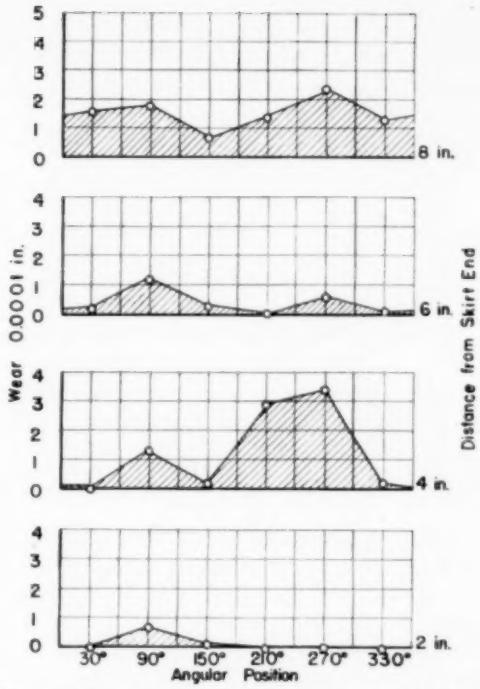

FIGURE 12.—*Wear in cylinder of radial aircraft engine.*

Secretary of Commerce. This company has developed a modification of the instrument for use with automobile engines under the trade name "McKee Wear Gage".[2]

The indentations used in this investigation were made by impressing into the test surface the apex of a four-sided diamond pyramid, which when viewed through the microscope was in the form of a sharp-pointed diamond. The chief limitation from the standpoint of accuracy was that the sharp points of the marks were blunted to some extent when wear occurred. A promising field for further work is to investigate the possibility of the use of cutting or grinding methods for producing marks without burrs and without sharp-pointed ends.

Acknowledgment is made to H. C. Dickinson, who instigated this investigation, and who, with C. E. Haven, F. A. Case, the late F. C. Knoop and other members of the Bureau staff, assisted in the development of the method.

WASHINGTON, May 5, 1947.

[2] Aminco–McKee Wear Gage, catalog 45, p. 208, American Instrument Co., Silver Spring, Md.

U. S. Department of Commerce
National Bureau of Standards

Research Paper RP1820
Volume 39, August 1947

Part of the Journal of Research of the National Bureau of Standards

Effect of Magnification on the Precision of Indoor Telescope Pointing

By Francis E. Washer

The principle variables affecting the precision of telescope pointing at an indoor target are magnification, brightness, and vernier acuity of the observer's eye. A series of experiments were performed in which magnification was the principle variable. All observations were made by a single observer, thus reducing variation in the vernier acuity. The brightness of the background against which the target was viewed was maintained at approximately the same level throughout the experiments to minimize effects arising from variation of brightness. Under these conditions, the relation between probable error of a single pointing (PE_s) and magnification (M) is approximately PE_s (in seconds) $= \frac{4.962}{M} + 0.068$.

I. Introduction

This study of the factors affecting the precision of telescope pointing was initiated in connection with the Range and Height Finder Development Project sponsored at the Bureau by the United States Army Ordnance. As a range finder is essentially a double-pointing instrument, it is possible to deduce the error that may be ascribed to the purely optical phase of the range finder system from the results obtained with a single telescope. The part of this investigation that deals with the precision of pointing for outdoor targets has already been reported [1, 2][1]

In this earlier investigation, no consideration was given to factors that may affect the probable error of a single pointing (PE_s) other than the distance separating target and observer. Other workers in this field have, however, devoted a great deal of attention to the correlation of PE_s with magnification of the observing telescope. The results of these attempts showed such wide discrepancies from one observer to another that it seemed worthwhile to investigate this matter further under carefully controlled conditions.

As control of conditions for outdoor pointing is not practicable, and as experience has shown that low and consistent values of PE_s are obtained indoors, the present study is made for indoor targets only. It must be emphasized that the term "pointing," as used in this paper, refers to a type of pointing where all mechanical errors have been eliminated and the error of pointing found is an attribute of the combination of the optical system and observer only, and is wholly devoid of such errors that may result from incorrect reading of verniers and scales such as exist on transit circles and similar mechanical devices. In addition, the term PE_s refers to the probable error of a single pointing about the instantaneous "true" pointing at the time at which it is made, and is a measure of the error of a single pointing determined from a number of pointings taken rapidly, and does not contain any appreciable effect of drift.

In planning an investigation into the effect of magnification on pointing accuracy, it is clear that there are many variables that must either be controlled or allowed to affect the results in whatever manner they may. For example, if the target and reticle size are kept unchanged and the magnification varied then the apparent width of target and reticle increases directly as the magnification. That this change in apparent width may be expected to have some effect is evidenced by some work done by Guild dealing with errors of optical settings [3]. His work was done with the unaided eye and showed appreciable variation for crossline widths varying from 10 to 180 seconds with the greatest change taking place between 10 and

[1] Figures in brackets indicate the literature references at the end of this paper.

748313—47——3

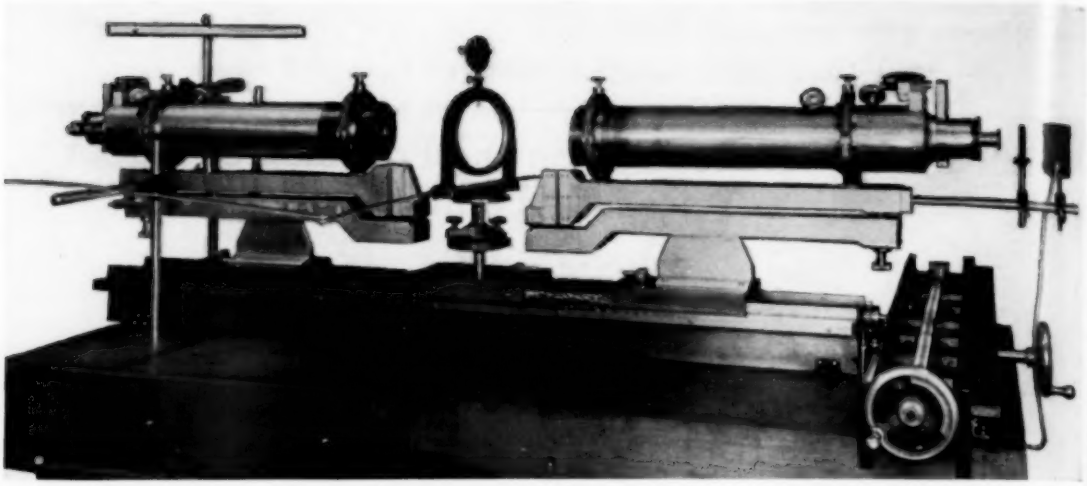

FIGURE 1.—*Arrangement of telescope, collimator, and rotating prism as used in the experiment.*

40 seconds. It is therefore possible that the value of PE_s for low magnifications may be influenced somewhat by the variation of apparent line widths. However, it was decided to omit control of this factor because the major portion of a given series of observations is taken under conditions where the apparent line width is over 40 seconds and hence in the region of very slow change.

A second factor that may affect the probable error of pointing is the apparent brightness of the background against which the target is viewed. This effect is discussed by Pelzer [4], who ascribes to it an importance out of proportion to its effect, in the opinion of the present author. This opinion is based on unpublished work in which it is found that while there is a slow increase in PE_s as one proceeds from a brightness so high as to be barely tolerable to a brightness lower by a factor of 1,000, the magnitude of this change can be neglected as long as the brightness is maintained at a level compatible with easy seeing. At very low brightnesses, there is a rapid increase in PE_s with diminishing brightness. However, this second factor was controlled during the present experiments so that the apparent brightness of the background against which the target is viewed was kept approximately constant at a level of easy seeing throughout this part of the work.

II. Apparatus and Method of Measurement

The apparatus and method of measurement are essentially the same as those described in the study of outdoor pointing accuracy [1]. The differences are primarily those concerned with size of telescope and auxiliary equipment. Two telescopes are used, one having an objective of 711-mm focal length and 100-mm aperture, and the second having an objective of 1,143-mm focal length and 50-mm aperture. The arrangement for the telescope with objective of 711-mm focal length is shown in figure 1. The collimator has an objective of 711-mm focal length and 100-mm aperture. The weak prism has 150-mm clear aperture, and the angle between its surfaces is 4 minutes.

To vary the pointing without disturbing the viewing telescope, the weak prism is placed in front of the telescope objective and so mounted that it may be rotated about a vertical axis, which is also parallel to the prism axis. As the deviation of a parallel beam of light caused by a weak prism is a function of the angle of incidence on the prism surface, the image of the target can be caused to move from side-to-side of the telescope cross-hair intersection by oscillating the prism. During the course of an observation the prism is rotated until

the image of the target appears to coincide with the cross-hair in the telescope, and the angular position of the prism is noted with the aid of an auxiliary telescope and scale in conjunction with a mirror attached to the rotating prism. This reading is converted into seconds in the object space. A series of ten such observations is taken and the probable errors, PE_s, determined from these data. Five such 10-groups are usually taken in a single run with a short intermission between each 10-group, and the average PE_s is accepted as the value of PE_s for the run.

All observations and the recording of data are performed by a single observer, the author, which, together with the fact that the rotation of the prism is controlled by a smooth rod that must be released between observations, acts to reduce any effect of memory in making successive settings, and so tends to ensure the independence of successive observations.

The probable error of a single pointing, PE_s, is computed from the approximate formula

$$PE_s \text{ (in seconds)} = \frac{0.8453k\sum_1^n |x_i - \overline{x}|}{\sqrt{n(n-1)}}, \qquad (1)$$

where $x_1, x_2, \ldots x_i \ldots x_n$ denote the n observations of a group and $\overline{x} = \frac{\sum x_i}{n}$ is the arithmetic mean of the n readings, and k is the calibration constant of the prism for conversion of millimeters observed on the scale to seconds deviation of the light beam caused by the prism. The observations are considered 10 at a time, and for $n=10$, eq 1 can be written

$$PE_s = 0.0891k\sum_1^{10} |x_i - \overline{x}|. \qquad (2)$$

The magnifications, 6, 12, 25.5, and 48 are obtained by four ocular lenses specially designed for use with the 711-mm telescope objective. Other magnifications, for the most part greater, are obtained by using a compound microscope as an ocular. By suitable choice of microscope objectives and oculars a wide range of magnifications is provided. The magnifications of the telescope with the four oculars are determined by two methods, first by the ratio of the focal length of the telescope objective to that of the ocular, and second by the ratio of entrance pupil to exit pupil with the telescope focused for parallel light, a condition that prevails throughout the experiment. For the four oculars the agreement by these two methods is good.

When microscopes are used as oculars, the total telescope magnification, M, is computed from the relation $M = m_1 \times m_2$, where m_1 is the objective magnification and m_2 the magnifying power of the microscope. The value of m_1 is given by the ratio of the focal length of the telescope objective to the distance of distinct vision, 250 mm. To insure against the errors that may result from accepting the nominal values of magnifying power of a microscope, each of the values of m_2 is carefully determined by experiment.

III. Results of Measurements

1. Spider Fiber as Target and 711-mm Objective in Viewing Telescope

The target is a spider fiber mounted in a vertical position in the focal plane of the collimator. The diameter of the spider fiber is approximately 4 μ; accordingly its diameter subtends an angle of approximately 1.3 seconds at the objective of the collimating telescope. This value of 1.3 seconds is nearly equal to the resolving power (1.2 seconds) of the observing telescope. The bright background, against which the spider fiber is viewed, is provided by a ground glass screen illuminated by a 6-v projection lamp. The brightness of the screen is varied when necessary by interposing neutral filters between the lamp and screen. The reticle in the observing telescope consists of two platinum wires 0.0001 in. in diameter intersecting at 90 degrees, this reticle being oriented to present the appearance of an $\times$. For the magnifications used, the apparent angular width of the spider hair ranges from approximately 8 to 329 seconds, while the apparent angular width of the reticle wires ranges from 5 to 227 seconds.

The results of measurement are listed in table 1 and shown graphically in figure 2. The form of the curve of PE_s versus magnification is an hyperbola, as is shown in figure 3, by plotting PE_s against the reciprocal of magnification. The straight line curve so obtained has a definite intercept on the PE_s axis at $\frac{1}{M}=0$ instead of passing through zero as might be expected.

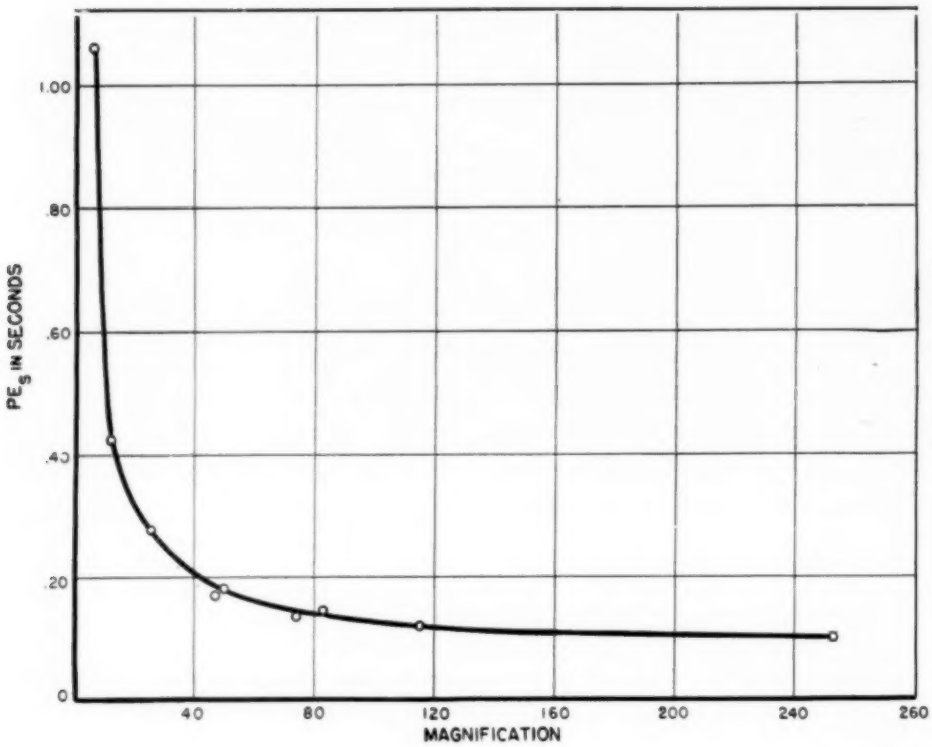

FIGURE 2.—*PE_s versus magnification.*

The results are for a viewing telescope with an objective of 711-mm focal length, 100-mm aperture. A spider fiber of approximately 4μ diameter mounted in the focal plane of the collimator is the target.

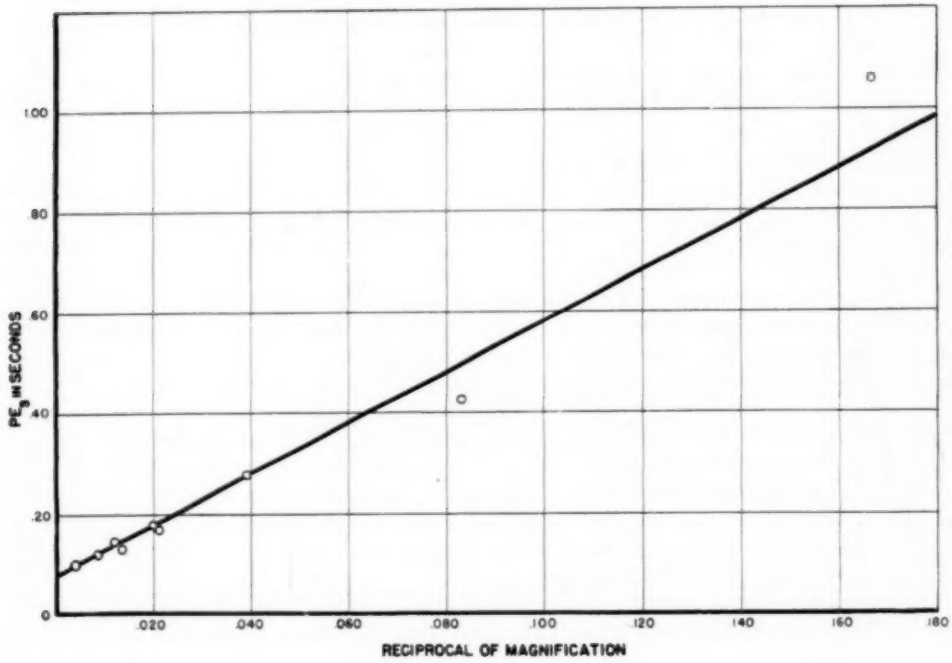

FIGURE 3.—*PE versus reciproc of magnificatio*

The results are fo a viewing telescop with an objective 711-mm focal length 100-mm aperture. A spider fiber of appro imately 4μ diamete mounted in the foc plane of the collimat is the target.

Thus the relation connecting PE_s and magnification is of the form

$$PE_s=\frac{A}{M}+B, \qquad (3)$$

where A and B are constants, and M is the magnification. For the curve in figure 3, A is the slope of the curve, and B, the intercept on the PE_s axis. Although the values of A and B can be obtained directly from the curve, a more accurate evaluation is made by least-squares considering only those values of PE_s for $M=25.5$. The final equation is found to be

$$PE_s=\frac{5.033}{M}+0.076. \qquad (4)$$

The values of PE_s for magnifications 6 and 12 are omitted from the solution because they do not lie as near to the straight line curve as do the others. Moreover a least-squares solution, based on all observed values of PE_s, yields computed values of PE_s that in two instances differ from the observed values by four or more probable errors. The present solution yields computed values of PE_s that in only one instance differ from the observed values of PE_s by as much as three probable errors, and that instance is for magnification 12, which was not included in the solution.

These differences between observed values and those calculated from eq 4 are given in table 1 under the heading ΔPE_s. It is noteworthy that these values of ΔPE_s are approximately the same or less than the values of P_p, listed under the column headed 1, for all values of $M \geq 25.5$. Even for magnifications 6 and 12, the values of ΔPE_s are only 2 or 3 times the value of P_p. It can therefore be stated that the values of PE_s calculated from eq 4, give excellent agreement with the observed values for the range of magnifications used.

Three values of P_p are listed in the tables under the headings 1, 2, and 3. The values listed under 1 are obtained from the formula

$$P_p=\frac{\pm 2PE_s}{3\sqrt{2(n-1)}}, \qquad (5)$$

where n is the total number of observations. For the present work this expression is sufficiently well approximated by the formula

$$P_p=\frac{\pm PE_s}{2\sqrt{n}} \qquad (6)$$

TABLE 1.—*Probable error of a single pointing (PE_s) as a function of magnification (M)*

The results are for a viewing telescope with an objective of 711-mm focal length, 100-mm aperture. A spider fiber of approximately 4-μ diameter mounted in the focal plane of the collimator is the target.

Magnification	PE_s		ΔPE_s	P_p			Number of 10-groups
	Obs	Calc	Obs.−Calc.	1	2	3	
Diameters	*sec*	*sec*	*sec*	*sec*	*sec*	*sec*	
6	1.000	0.915	0.145	0.075	0.075	0.058	5
12	0.425	.495	−.070	.021	.030	.043	10
25.5	.277	.273	.004	.009	.020	.025	45
48	.170	.181	−.011	.012	.012	.004	5
50	.180	.177	.003	.009	.013	.012	10
74	.135	.144	−.009	.007	.010	.017	10
83	.145	.137	.008	.007	.010	.014	10
115	.120	.120	.000	.008	.008	.004	5
253	.100	.096	.004	.005	.007	.007	10

$PE_s=\frac{5.033}{M}+0.076$

The values of P_p, obtained by this formula, with n taken as the total number of observations, is especially useful for comparison with ΔPE_s, the difference between observed and calculated values of PE_s. The values of P_p, listed under 2, are obtained by use of the same formula, with PE_s the average value for five 10-groups and for $n=50$. Where there are several 50-sets involved, the value of P_p is the average for the several 50-sets, and represents what might be termed the average theoretical probable error of the probable error for five 10-groups. The value of P_p, listed under column 3, is obtained by considering each PE_s from a single 10-group as an observation and computing the probable error of the mean for the average value of PE_s from five 10-groups. Where more than one 50-set is considered, the value of P_p is the average for the several 50-sets. Ideally P_p, computed in this manner, should equal the value of P_p listed under column 2. It is noteworthy that fairly good agreement prevails between the values of P_p, listed under columns 2 and 3, for the same magnification.

2. Platinum Wire as Target and 711-mm Objective in Viewing Telescope

The target is a platinum wire mounted vertically in the focal plane of the collimator. The

diameter of the wire is 0.0005 in., which subtends an angle of 4 seconds at the objective. All other conditions of the experiment are essentially the same as those for the spider fiber as target.

The results of measurement are listed in table 2. Assuming the same form of equation connecting PE_s and magnification evaluation of the constants A and B by least-squares gives the relation

$$PE_s = \frac{5.262}{M} + 0.060, \tag{7}$$

which is nearly the same as eq 4 found for the spider-fiber target. A comparison of observed and calculated values of PE_s given in table 2

TABLE 2.—*Probable error of a single pointing (PE_s) as a function of magnification (M).*

The results are for viewing telescope with an objective of 711-mm focal length, 100-mm aperture. A platinum wire 0.0005-in. in diameter mounted in the focal plane of the collimator is the target.

Magnification	PE_s		ΔPE_s	P_p			Number of 10-groups
	Obs.	Calc.	Obs.−Calc.	1	2	3	
Diameters	*sec*	*sec*	*sec*	*sec*	*sec*	*sec*	
6.9	0.942	0.937	0.005	0.033	0.067	0.082	20
19.6	.308	.328	−.020	.011	.022	.030	20
25.5	.270	.266	.004	.007	.020	.016	40
36.4	.192	.205	−.013	.007	.014	.014	20
50	.170	.165	.005	.008	.012	.011	10
83	.135	.123	.012	.007	.010	.010	10
115	.105	.106	−.001	.005	.008	.009	10
181	.087	.089	−.002	.004	.006	.006	10
223	.094	.084	.010	.005	.007	.012	10
253	.079	.081	−.002	.004	.006	.008	10
414	.070	.073	−.003	.004	.005	.005	10

$$PE_s = \frac{5.262}{M} + 0.060.$$

shows excellent agreement. The significance of ΔPE_s and the three values of P_p are the same as explained in section 1. The theoretical value of P_p, listed in column 2, shows very close agreement with the value of P_p determined from the spread of values of PE_s, listed under column 3.

3. Platinum wire as target and 1,143-mm objective in viewing telescope

In this part of the experiment, a telescope objective with focal length of 1,143-mm is used to study possible effect on the values of PE_s that may arise with change of focal length of the observing telescope objective. All other conditions remain the same as described in section 2.

The results of measurements are listed in table 3. Assuming that the form of the equation connecting PE_s and magnification is the same as eq 7, evaluation of the constants by least-squares gives the relation

$$PE_s = \frac{4.592}{M} + 0.067, \tag{8}$$

which closely resembles eq 4 and eq 7. A comparison of observed and calculated values given in table 3 shows excellent agreement.

TABLE 3.—*Probable error of a single pointing (PE_s) as a function of magnification (M).*

The results are for a viewing telescope with an objective of 1,143-mm focal length, aperture 50-mm. A platinum wire of 0.0005-in. in diameter mounted in the focal plane of the collimator is the target.

Magnification	PE_s		ΔPE_s	P_p			Number of 10-groups
	Obs.	Calc.	Obs.−Calc.	1	2	3	
Diameters	*sec*	*sec*	*sec*	*sec*	*sec*	*sec*	
26.5	0.239	0.240	−0.001	0.017	0.017	0.017	1
32.2	.208	.210	−.002	.015	.015	.024	1
49.1	.165	.161	.004	.012	.012	.017	1
134	.100	.101	−.001	.007	.007	.008	1
157	.099	.096	.003	.007	.007	.007	1
291	.079	.083	−.004	.006	.006	.012	1

$$PE_s = \frac{4.592}{M} + 0.067$$

IV. Discussion

Although the variation of probable error of telescope pointing with magnification has frequently been the subject of investigation [1], the results have been so diverse that it seemed worthwhile to study this phase of pointing accuracy with the present equipment. It seems probable that the wide variations in the results previously reported arise from the attempt to correlate PE_s with magnification for pointings made at an outdoor target without control of other variables. Such pointings are likely to be influenced by turbulence of the air intervening between observer and target, lighting conditions and degree of contrast, configuration or shape of the target viewed, arrangement and size of the cross-hairs in the observing telescope, and small movements of the observing telescope or the object viewed. In addition, some investigators have handicapped themselves at the outset by assuming that there should be a definite relation connecting pointing accuracy and resolving power of the telescope objective [6, 7, 8, and 9].

The possibility of such a relation is minimized by Tilton [10] who, in the course of some precise work on prism size, found it necessary to study the effect on pointing accuracy with change of aperture of objective. His findings indicate no significant change or pointing accuracy with resolving power. It is probable that a belief (not always definitely stated) that pointing accuracy does not differ greatly from the limit of resolving power influenced some investigators to be satisfied with a relatively coarse adjustment in making their settings. For example, Pelzer [4], the first worker to make definite attempts to control brightness, arrives at such high values of PE_s (varying from 0.9 to 1.4 seconds for magnifications varying from 28 to 14) that it appears very likely that he did not employ a sufficiently fine means of reading his pointings. Also, many observers appear to base their formulas relating magnification and pointing accuracy upon results obtained for relatively few magnifications. Thus, Noetzli [11], in his work on outdoor pointing, bases his equation

$$PE_s = \frac{2.7}{\sqrt{M}} \text{ to } \frac{2.0}{\sqrt{M}} \tag{9}$$

upon magnifications 12, 24, and 37, while Klempau [12] bases his equation

$$PE_s = \frac{4.9}{\sqrt{M}} \text{ to } \frac{3.0}{\sqrt{M}} \tag{10}$$

upon magnifications 19, 23, and 30.

One of the best pieces of work definitely dealing with indoor pointing accuracy is that by Noetzli [11]. He first investigates the effect of magnification upon pointing accuracy under conditions that preclude errors arising from the presence of cross-hairs in the ocular, and, for a range of magnification from 1 to 78, finds the relation [2]

$$PE_s = \frac{1.39}{M} \tag{11}$$

However, in making the settings in the second part of his investigation, wherein he used cross-hairs in the ocular, he gets the relation

$$PE_s = \frac{0.486}{\sqrt{M}}, \tag{12}$$

which is clearly open to question in view of the present study. In seeking an explanation for this discrepancy, the present author has plotted Noetzli's values in the form of $M \times PE_s$ versus M, which is shown in figure 4, for pointings both with and without cross-hairs. It is clear for those values of M in excess of 15.7 that Noetzli's values with cross-hairs fall on a curve satisfying the equation

$$M \times PE_s = 1.665 + 0.035M, \tag{13}$$

while those values of $M \times PE_s$ found for M varying from 1 to 8.6 not only fall well below this curve, but they also are lower than the corresponding values of $M \times PE_s$ for all magnifications without cross-hairs. It seems very improbable that the pointings with cross-hairs should be better than the pointings without cross-hairs for magnifications 1 to 8.6 and inferior for magnifications in excess of 15.7. It is noteworthy that these discrepancies are pronounced only for the lower magnification where, according to table 1 in Noetzli's paper, a telescope objective was used as ocular. Whenever long focal length lenses are used as oculars, it is possible that there may be sufficient difference in adjustment of objective and ocular (or of the reticle with respect to the objective and ocular) to produce a difference in magnification between the condition of pointing with and without cross-hairs. The tendency for the normal observer would be toward an adjustment producing a higher magnification for pointings with than for those without cross-hairs. Accordingly, the magnifications 1 to 8.6, listed by Noetzli, may actually have been somewhat higher for the condition of pointing with cross-hairs that they were without cross-hairs.

When eq 13 is transformed into the equivalent form

$$PE_s = \frac{1.65}{M} + 0.035, \tag{14}$$

which is identical with the form in eq 1, it is clear that the constant B is not appreciably different from the average value of 0.068 found in the present experiment. The value A is, however, very much smaller than the value of 4.962 reported here. Since, however, the constant A is the vernier acuity of the observer's eye, and there is considerable variation in this quantity from one

[2] The constants in Noetzli's equations have been adjusted by the present author to express probable error instead of root-mean-square error.

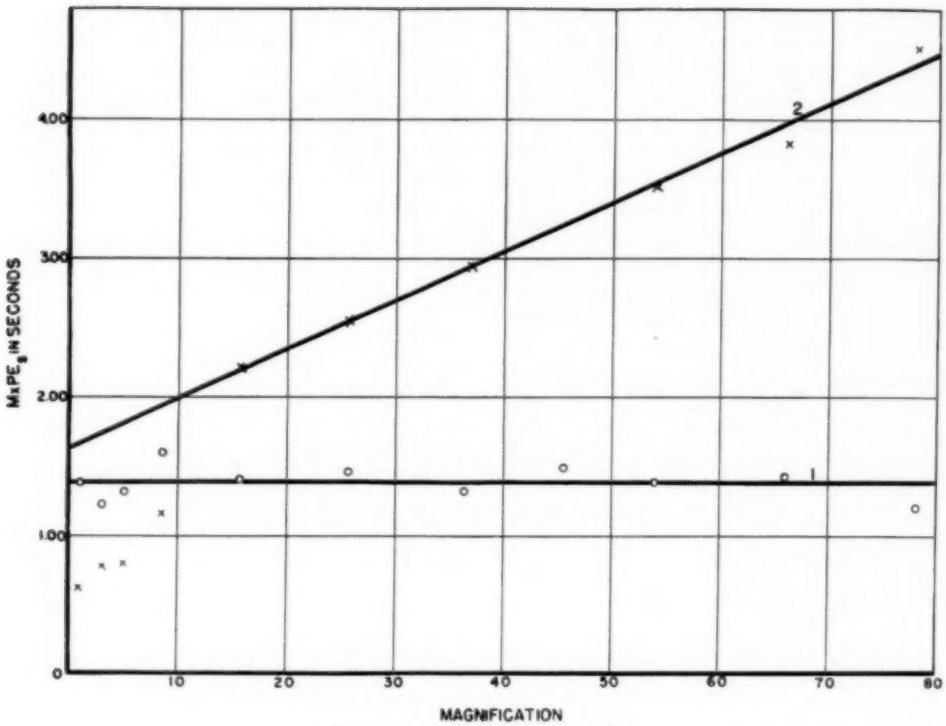

FIGURE 4.—$M \times PE_s$ *versus* M.

Observed values of $M \times PE_s$ with cross-hairs are indicated by crosses; curve 2 shows the theoretical curve for $M > 15.7$. Observed values of $M \times PE_s$ without cross-hairs are indicated by circles; curve 1 shows the theoretical curve. These results are obtained from Noetzli's paper. (See reference [11]).

observer to another, the differences in the constant A introduce no difficulty.

V. Conclusion

The relation between PE_s and magnification is found from this experiment to be expressible in the form

$$PE_s = \frac{A}{M} + B,$$

where A and B are constants. On averaging the values of A and B for the three cases described, the resulting equation is

$$PE_s = \frac{4.962}{M} + 0.068 \qquad (15)$$

It is problematical whether any significance can be attached to the variation of the constants A and B for the three cases. This question can only be answered by further study where a wider range of target diameters and focal lengths of the observing telescope are used. The constant A is the vernier acuity of the observer's eye and can undoubtedly be expected to vary from one observer to another. The value of 4.96 seconds is within the range of values obtained by different observers, contained in a discussion of vernier acuity in a paper by Walls [13].

It is more difficult to account for the constant B. Previous workers in this field have used equations in which A only appeared, PE_s being correlated with the reciprocal of magnification. Two possibilities are here advanced in interpretation of the constant B. The first is vibration that is always present however much it may be reduced by careful mounting. The second possibility is that the short air column separating the collimator and telescope objective may by its turbulence introduce the additional error represented in the equation by B. In the study of

outdoor pointing, the possibility of a dependence of pointing accuracy upon range was discussed [1]. The contribution dependent on range was given as $0.064d^{\frac{1}{2}}$ where d is the range in meters. The distance separating the collimator and telescope objective in this experiment was approximately 0.75 meter. Accordingly the computed error arising from range is approximately 0.059 second, which is not significantly different from the values of B found in the present experiment on indoor pointing.

VI. References

[1] F. E. Washer and H. B. Williams, Precision of telescope pointing for outdoor targets. J. Optical Soc. Am. **36,** 400 (1946).

[2] F. E. Washer and H. B. Williams, precision of telescope pointing for outdoor targets. J. Research NBS **36,** 479 (1946) RP1717.

[3] J. Guild, The insensitivity and personal equation errors of optical settings. Trans. Optical Soc., (London) **31,** 1 (1929–30).

[4] A. Pelzer, Uber den Einfluss der Lichtstarke von Theodolit- und Nivellier-fernrohren auf den mittleren Zielfehler, Z. Instrumentenk. **46,** 354 (1926).

[5] A. G. Worthing and J. Geffner, Treatment of experimental data, p. 197 (John Wiley & Sons, Inc., New York, N. Y., 1943).

[6] A. A. Michelson, Measurement by light-waves. Am. J. Sci. **39,** 115 (1890).

[7] A. A. Michelson, Light-waves and their application to metrology. Nature **49,** 56 (1893–94).

[8] F. L. O. Wadsworth, On the conditions which determine the ultimate optical efficiency of methods for observing small rotations. Phil. Mag. **44,** 83 (1897).

[9] F. L. O. Wadsworth, On the optical conditions required to secure maximum accuracy of measurement in the use of telescopes and spectroscope. Astrophys. J. **16,** 267 (1902).

[10] L. W. Tilton, Prism size and orientation in minimum deviation refractometry. BS J. Research **6,** 59 (1931) RP262.

[11] A. Noetzli, Untersuchung uber die Genauigkeit des Zielens mit Fernrohren. Z. Instrumentenk. **35,** 65 and 89, (1915).

[12] Fr. Klempau, Uber die Beziehungen zwischen Winkel-Nonien-, und Zielgenauigkeit, Allgem. Verm.-Nachr. **25,** 317 (1923).

[13] G. L. Walls, Factors in human visual resolution, J. Optical Soc. Am. **33,** 487 (1943).

WASHINGTON, October 2, 1946

U. S. Department of Commerce
National Bureau of Standards

Research Paper RP1821
Volume 39, August 1947

Part of the Journal of Research of the National Bureau of Standards

Heats of Formation and Isomerization of the Eight C_8H_{12} Alkylcyclohexanes in the Liquid and Gaseous States[1,2]

By Edward J. Prosen, Walter H. Johnson, and Frederick D. Rossini

From experimental data recently obtained on the heats of combustion of the eight C_8H_{16} alkylcyclohexanes in the liquid state at 25° C, together with auxiliary data on the differences in the heats of vaporization at 25° C and on the difference in heat content of the gas between 0° K and 25° C, values are calculated for the following properties: the heat of isomerization of ethylcyclohexane into the given dimethylcyclohexane in the gas state at 25° C, and also in the gas state at 0° K; the heat of formation, from the elements, of the given isomer in both the liquid and gas states at 25° C and in the gas state at 0° K. The relation of the energy content to the structure of these molecules is discussed, including the labeling of the lower and higher-boiling forms of 1,3-dimethylcyclohexane as *cis* and *trans*, respectively.

I. Introduction

Values were recently reported for the heats of formation of the normal alkylcyclopentanes and normal alkylcyclohexanes [1].[3] This report presents values of the heats of formation, for the gaseous and liquid states, and isomerization, for the gaseous state, of the eight C_8H_{16} alkylcyclohexanes, based on the results of measurements recently reported [2] on the heats of combustion of the eight C_8H_{16} alkylcyclohexanes in the liquid state at 25° C.

II. Results

The results of the present calculations are given in table 1. The values in column 2 are the results of the measurements of the heats of isomerization at 25° C in the liquid state [2]. These measurements were made in a manner similar to that previously reported for the eight C_9H_{12} alkylbenzenes at 25° C in the liquid state [3]. The values in column 3 are the differences in the heats of vaporization at 25° C, with the gas in the thermodynamic standard state of unit fugacity [4.] The values in column 4 are the heats of isomerization at 25° C in the gaseous state, obtained by combining the values in columns 2 and 3. The values in columns 5 and 6 give the heats of formation, from the elements, solid carbon (graphite) and gaseous hydrogen, for the C_8H_{16} alkylcyclohexanes in the liquid and gaseous standard states, respectively. These values were obtained by combining the values previously reported for the heats of formation of gaseous and liquid ethylcyclohexane [1] with the values of the heats of isomerization given in columns 2 and 4.

Column 7 gives the differences of the values of the heat content at 298.16° K less that at 0° K for these compounds in the standard gaseous state [5]. The values in column 8 give the heats of isomerization at 0° K for the standard gaseous state, obtained by combining the values in columns 4 and 7. The values in column 9 give the heats of formation, from elements, solid carbon (graphite) and gaseous hydrogen, for the hydrocarbon in the standard gaseous state at 0° K. The value for the heat of formation of ethylcyclohexane in the standard gaseous state at 0° K was obtained from the corresponding value for 25° C, in column 6, and the values for the heat content at 298.16° K less that at 0° K for gaseous ethylcyclohexane [5], solid carbon (graphite) [6], and gaseous hydrogen [6].

[1] This investigation was performed at the National Bureau of Standards jointly by the Thermochemical Laboratory and the American Petroleum Institute Research Project 44.

[2] Presented before the Division of Physical and Inorganic Chemistry of the American Chemical Society at Atlantic City, N. J., April, 1947.

[3] Figures in brackets indicate the literature references at the end of this paper.

TABLE 1.—*Values of the heats of isomerization and formation of the C_8H_{16} alkylcyclohexanes*

Compound	$\Delta Hf°$ (isomerization) for the liquid state at 25° C [a]	Difference in the heats of vaporization at 25° C [d]	$\Delta Hf°$ (isomerization) for the gaseous state at 25° C [e]	$\Delta Hf°$ (liquid) at 25° C [f]	$\Delta Hf°$ (gas) at 25° C [g]	Difference in $(H°_{298.16}-H°_0)$ for the gaseous state [h]	$\Delta Hf°$ (isomerization) for the gaseous state at 0° K [e]	$\Delta Hf°$ (gas) at 0° K [g]
	kcal/mole	*kcal/mole*	*kcal/mole*	*kcal/mole*	*kcal/mole*	*kcal/mole*	*kcal/mole*	*kcal/mole*
Ethylcyclohexane	0.00	0.00	0.00	−30.72±0.37	−41.05±0.37	0.00	0.00	−28.94±0.38
1,1-Dimethylcyclohexane	−1.58±0.28	−0.63±0.04	−2.21±0.28	−52.30±0.46	−43.26±0.46	−0.22±0.01	−1.99±0.28	−30.93±.47
cis-1,2-Dimethylcyclohexane	−0.08±0.25	−.18±.01	−0.10±.25	−50.64±.45	−41.15±.45	−.09±0.01	−0.01±.25	−28.95±.46
trans-1,2-Dimethylcyclohexane	−1.46±0.27	−.51±.01	−1.97±.27	−52.18±.46	−43.02±.46	−.00±0.01	−1.97±.27	−30.91±.47
cis-1,3-Dimethylcyclohexane [a]	−2.57±0.22	−.54±.01	−3.11±.22	−53.29±.43	−44.16±.43	−.03±0.01	−3.08±.22	−32.02±.44
trans-1,3-Dimethylcyclohexane [b]	−0.85±0.21	−.30±.01	−1.15±.21	−51.57±.43	−42.20±.43	−.03±0.01	−1.12±.21	−30.06±.43
cis-1,4-Dimethylcyclohexane	−0.83±.21	−.34±.01	−1.17±.21	−51.55±.43	−42.22±.43	−.03±0.01	−1.14±.21	−30.08±.43
trans-1,4-Dimethylcyclohexane	−2.45±.22	−.62±.01	−3.07±.22	−53.17±.43	−44.12±.43	−.02±0.01	−3.05±.22	−31.99±.44

[a] This isomer, formerly labeled "*trans*", has the following properties [7]: boiling point at 1 atm, 120.09°C; refractive index, n_D at 25° C, 1.4206; density at 25° C, 0.7620 g/ml.

[b] This isomer, formerly labeled "*cis*", has the following properties [7]: boiling point at 1 atm, 124.45°C; refractive index, n_D at 25° C, 1.4284; density at 25° C, 0.7806 g/ml.

[c] Heat of isomerization of ethylcyclohexane into each of the dimethylcyclohexanes, $H°$ (dimethylcyclohexane, liquid) $-H°$ (ethylcyclohexane, liquid) at 25° C.

[d] The difference in the standard heats of vaporization, $[H°$ (gas) $-H°$ (liquid)] (dimethylcyclohexane) $-[H°$ (gas) $-H°$ (liquid)] (ethylcyclohexane) at 25° C.

[e] Heat of isomerization of ethylcyclohexane into each of the dimethylcyclohexanes, $H°$ (dimethylcyclohexane, gas) $-H°$ (ethylcyclohexane, gas) at the temperature stated.

[f] Heat of formation, for the reaction 8 C (solid, graphite) $+8H_2(gas)=C_8H_{16}$ (liquid, alkylcyclohexane), with each reactant and product in its standard state at 25° C.

[g] Heat of formation, for the reaction 8 C (solid, graphite) $+8H_2(gas)=C_8H_{16}$ (gas, alkylcyclohexane), with each reactant and product in its standard state at the temperature stated.

[h] $[H°_{298.16}-H°_0]$ (gas, dimethylcyclohexane) $-[H°_{298.16}-H°_0]$ (gas ethylcyclohexane).

The remaining values were obtained by combining this with the values in column 8. In table 1, the lower-boiling isomer, formerly labeled *trans*, is labeled *cis*, and the higher-boiling isomer, formerly labeled *cis*, is labeled *trans* [7], following the reasoning originally presented by Pitzer and Beckett [8] and confirmed here by the values of the differences in energy content.

III. Discussion

Pitzer and Beckett [8] have summarized in detail the possible configurations of the substituted cyclohexanes, showing that at ordinary temperatures substantially all of the molecules are in the "chair" configuration of the cyclohexane nucleus. In the cyclohexane ring in this configuration, each carbon atom is staggered alternately above and below a plane through the ring of carbon atoms, with the results that six of the substituents to the ring (hydrogen atoms or methyl groups) are in an "equatorial" belt around the ring, while three substituents are north "polar" above the ring, and three are south "polar" below the ring. If the six carbon atoms in the ring are twisted simultaneously so that the staggering with respect to the plane through the ring of carbon atoms is reversed, the six substituents that were originally equatorial become polar (three north and three south), while those that were polar become equatorial. When one or more of the substituents on different carbon atoms are different, the inversion produces tautomers, and Pitzer and Beckett [8] give in detail the number and description of such tautomers for the several dimethylcyclohexanes. For example, in the case of *trans*-1,4-dimethylcyclohexane, one tautomer has both methyl groups polar and the other has both methyl groups equatorial. The tautomer with the methyl groups polar will possess a considerable amount of steric or strain energy (estimated by Pitzer and Beckett [8] to be near 4 kcal/mole) over that of the tautomer with both methyl groups equatorial, and the population of the higher energy state will be very small at ordinary temperatures.

For consideration of the relation between energy content and molecular structure, the values of energy content for the gaseous state at 0° K are preferably used, because all of the molecules of a given isomer will then be in the tautomeric state of lower energy, as well as being in the ground states, for translational, rotational, and ordinary vibrational energy. In the case of the example cited above, *trans*-1,4-dimethylcyclohexane, all of the molecules will be in the more stable tautomeric state with both methyl groups equatorial.

The conclusions reached by Pitzer and Beckett [8] together with the results of the present calculations, are summarized in table 2. The extraordinary accord of the values in the last two columns is to be noted. The difference in energy due to a

change of methyl group from an equatorial to a polar position, which is 2a according to Pitzer's [9] theoretical calculations, is evaluated from the experimental data to be 1.94 ± 0.10 kcal/mole.

TABLE 2.—*Dimethylcyclohexanes in their more stable tautomeric forms, in the gaseous state at 0° K*

Isomer	Position of the two substituents in the more stable tautomeric form (*e*, equatorial; *p*, polar) [8]	Theoretical strain energy (referred to two equatorial groups on nonadjacent carbon atoms as zero) (from Pitzer and Beckett, [8]).	Experimental difference in energy content[a] (referred to two equatorial groups on nonadjacent carbon atoms as zero)
			kcal/mole
cis-1,2-Dimethylcyclohexane	*e, p*	3a	3.04±0.21
trans-1,2-Dimethylcyclohexane	*e, e*	a	1.08± .23
cis-1,3-Dimethylcyclohexane[a]	*e, e*	0	−0.03± .17
trans-1,3-Dimethylcyclohaxane[b]	*e, p*	2a	1.93± .15
cis-1,4-Dimethylcyclohexane	*e, p*	2a	1.91± .15
trans-1,4-Dimethylcyclohexane	*e, e*	0	0.00

[a] Formerly labeled "*trans*," see footnote a of table 1.
[b] Formerly labeled "*cis*," see footnote b of table 1.
[c] Includes the calculated correction (column 7 of table 1) from 25° C to 0° K.

The above considerations on energy content follow the conclusions originally reached by Pitzer and Beckett [8] and require that, among the 1,3–dimethylcyclohexanes, the isomer having the lower energy content be the "*cis*" isomer and that having the higher energy content be the "*trans*" isomer. These designations require a reversal of the previous labeling of these two isomers, so that the lower boiling isomer formerly labeled *trans*, is now labeled *cis*, and the higher-boiling isomer, formerly labeled *cis*, is now labeled *trans* [10].

IV. References

[1] E. J. Prosen, W. H. Johnson, and F. D. Rossini, J. Research NBS **37,** 1 (1946) RP1728.

[2] W. H. Johnson, E. J. Prosen, and F. D. Rossini, J. Research NBS **39, 49** (1947) RP1812.

[3] W. H. Johnson, E. J. Prosen, and F. D. Rossini, J. Research NBS **35,** 141 (1945) RP1665.

[4] American Petroleum Institute Research Project 44 at the National Bureau of Standards. Table 7q. Standard heat, entropy, and free energy of vaporization at 25° C (March 31, 1947).

[5] C. W. Beckett, K. S. Pitzer, and R. Spitzer, J. Am. Chem. Soc. **69** (Aug. 1947).

[6] D. D. Wagman, J. E. Kilpatrick, W. J. Taylor, K. S. Pitzer, and F. D. Rossini, J. Research NBS **34,** 143 (1945) RP1634.

[7] American Petroleum Institute Research Project 44 at the National Bureau of Standards. Table 7a. Boiling point, density, refractive index, and freezing point. (March 31, 1947.)

[8] K. S. Pitzer and C. W. Beckett, J. Am. Chem. Soc. **69,** 977 (1947).

[9] K. S. Pitzer, J. Chem. Phys. **8,** 711 (1940).

[10] F. D. Rossini and K. S. Pitzer, Science **105, 647** (1947).

WASHINGTON, March 1, 1947

U. S. Department of Commerce
National Bureau of Standards

Research Paper RP1822
Volume 39, August 1947

Part of the Journal of Research of the National Bureau of Standards

Some Recent Advances in Our Understanding of the Chemistry of Portland Cement

By Robert H. Bogue

A review is given of some of the more important advances that have been made in our understanding of portland cement during the war years, or more specifically from 1942 to 1946. The field covered is limited strictly to chemical research, and no attempt is made to include more than the outstanding contributions. The presentation is given of thirteen investigational fields of study, classified in four major divisions. The more significant results are brought together in a summary.

I. Notation

The commonly used abbreviated symbols for the cement components are used interchangeably with the conventional notation. Thus, C-CaO, S-SiO_2, A-Al_2O_3, F-Fe_2O_3, H-H_2O, N-Na_2O, K-K_2O, M-MgO. Hence, C_2AH_x-$2CaO.Al_2O_3.8H_2O$, etc.

II. Introduction

Since the close of the war, scientists from countries throughout the world have been concerned with catching up on the progress made in other countries during the years when communication was barred. In our laboratories, as in others, our friends seek to learn of the advances that have come from chemical research on portland cement. The answer is not to be found in any one place. To meet that need is one of the purposes of this paper.

No attempt is made at a comprehensive picture. Only a few of the more significant studies can be presented, and these are confined to the strictly chemical fields. A more extensive treatment has recently been published elsewhere [1].[1] Many important advances likewise have been made in the fields of physics, engineering, manufacture, architecture, etc. But what we see in our own field gives promise of a most interesting future. The treatment will be directed to a review of research on phase composition, crystal structure, reactions of hydration, and new technics.

[1] Figures in brackets indicate the literature references at the end of this paper.

III. Phase Composition of Clinker

Recent work upon the phase composition of portland cement clinker has given new information along several important directions.

1. Combinations of Potash

Although the alkalies in cement are probably never present in amounts exceeding 2 percent, and usually their total is under 1 percent, yet their presence in even smaller quantities is known to produce effects which, under certain conditions, are the subject of concern. One observed effect [12] is that increasing amounts of alkali in the mix result in increased difficulty, during manufacture, in keeping down the free CaO. Another [36] is the undue expansion of high-alkali cements with certain types of siliceous aggregates. In order to understand the action of the alkalies in cement, it is essential to know the forms in which these elements exist in clinker, and the phase relations by which they may be controlled.

In a study of the system K_2O—CaO—Al_2O_3, Brownmiller [5] found that only one compound of potash was formed which could exist in the general composition-range of portland cement. This was the binary compound KA. Taylor [39] showed later that this compound was stable in the presence of the iron compound of cement, C_4AF. The latter compound was known to form a solid solution with C_2F [13], and this solid solution was found to act as a pseudobinary system with the

KA. The next step was to examine the effects resulting from the addition of the calcium silicates. This study [40] showed that KA reacts with C_2S and C_3S to form a potash-lime-silica compound of the composition $KC_{23}S_{12}$.

Further investigation [41] revealed that the new ternary compound is stable in the presence of C_3A, C_4AF, C_3S, C_2S and MgO. Hence it would be the stable potash-containing phase in the cement area of the system K_2O—CaO—MgO—Al_2O_3—Fe_2O_3—SiO_2. On an exploration of the system CaO—$KC_{23}S_{12}$—C_3A_3, a quintuple invariant point was found where $KC_{23}S_{12}$, C_3A and C_5A_3 are in equilibrium with liquid and vapor at 1,310° C. Likewise, a quintuple point, not a eutectic, was found for the phases $KC_{23}S_{12}$, CaO and C_3A at a temperature of 1,450° C.

The discovery of the ternary potash-lime-silica compound, stable in cement systems of the above six components, explains why the addition of potash to a raw mix may result in progressively increasing amounts of free CaO in the clinker. Thus it may be computed that 1 percent of potash combines with 21.9 percent of C_2S to form 22.3 percent of $KC_{23}S_{12}$, with the liberation of 0.6 percent of CaO, by the equation

$$K+12C_2S \longrightarrow KC_{23}S_{12}+C.$$

This 0.6 percent of CaO can combine with 1.9 percent of C_2S to form 2.5 percent of C_3S by the equation

$$C+C_2S \longrightarrow C_3S$$

so that a total of 23.8 percent of C_2S will have been removed by the introduction of the 1 percent of K_2O. But if the mixture had a potential C_2S content less than 23.8 percent, the liberated CaO could not all be combined and would remain as free CaO in the clinker. When 1 percent of K_2O reacts with C_3S, 29.1 percent of the latter will be combined, with the liberation of 7.7 percent of CaO, by the equation

$$K+12C_3S \longrightarrow KC_{23}S_{12}+13C.$$

Before these data could be applied directly to portland cement compositions, it was necessary to examine the effect of SO_3 on the potash compound. It was found that the introduction in the raw mix of SO_3 in the form of $CaSO_4$ brought about a reaction with the $KC_{23}S_{12}$ by which C_2S and K_2SO_4 were produced, in accordance with the equation

$$KC_{23}S_{12}+CaSO_4 \longrightarrow 12C_2S+K_2SO_4.$$

Additional tests showed that, in clinker compositions, the SO_3 and K_2O combine preferentially as K_2SO_4, which crystallizes readily. To the extent that SO_3 is available, the potash will combine with it, and only the excess of K_2O will combine as $KC_{23}S_{12}$. In most clinkers examined it was found that the K_2O is in excess of its molecular equivalent of SO_3, which would suggest the probability that the potash is present in both of the above compounds. A microscopical search for K_2SO_4 in clinkers revealed its presence in more than half of those examined. It could usually be found when the calculated potential K_2SO_4 content exceeded 0.24 percent. The existence of K_2SO_4 in clinker had previously been indicated by microscopical [4] and chemical [23] studies.

2. Combinations of Soda

The soda systems have been studied in much the same manner as the potash systems. It was learned [6] in 1932 that a soda compound is formed in the system Na_2O—CaO—Al_2O_3, in the region of portland cement, having the composition NC_8A_3. This compound was found to be stable in the presence of C_3A, but it was necessary, as a next step, to examine its stability in the presence of the calcium silicates.

This was accomplished [11] in 1946 through the study of a portion of the quaternary system Na_2O—CaO—Al_2O_3—SiO_2, which would include the compounds NC_8A_3, C_3A, C_3S and C_2S. For this purpose, a secondary system was selected within the larger system, having as components, CaO, C_2S, NA and Al_2O_3. This system, represented diagramatically as a tetrahedron, was examined by taking compositions along three planes, each of which hinged on the CaO—C_2S axis, but met the Al_2O_3—NA axis at different points. These planes could then be represented as the pseudo-ternary systems,

$$C_2S-CaO-(Na_2O+6Al_2O_3)$$
$$C_2S-CaO-(Na_2O+3Al_2O_3)$$
$$C_2S-CaO-NA$$

The first two planes are only arbitrary sections and do not represent true ternary systems, but the last plane is a true ternary system. In the pseudo-ternary systems, the compositions of liquids and crystalline phases encountered are likely to lie outside the plane, and the course of crystallization

could not be followed from the ternary diagram. But by separate explorations in critical regions between the planes, the necessary data could be obtained.

Of especial importance, it was found that NC_8A_3 could exist in stable equilibrium with C_3A, C_2S, and C_2S in the region of the system approaching portland cement in composition. An invariant point of those four crystalline compounds with liquid was found at 1,440° C. This means that, on heating such a mixture, liquid would first appear at that temperature, and would have the determined composition of the invariant-point liquid. It appeared from microscopical and X-ray data that the NC_8A_3 and C_3A might combine, at temperatures below that of liquid formation, to form a solid-solution series. Also, under certain conditions, it appeared that the C_2S crystallized out in the α rather than in the β modification, and in that form was able to take up a small amount of soda in solid solution. But when the α C_2S inverted to the β form, the soda phase, being less soluble in the latter modification of the dicalcium silicate, came out of solution and appeared as inclusions in the βC_2S crystals.

It may be concluded from this study that soda may exist in a mixture of the components Na_2O, CaO, Al_2O_3, and SiO_2 in one or more of four forms:

1. As a component of glass,
2. As NC_8A_3 or a solid solution of that phase in C_3A,
3. As a solid solution of a soda-bearing phase in α C_2S,
4. As inclusions of a soda-bearing phase in β C_2S produced by ex-solution on inversion of the α C_2S.

The amount of soda in the glass will depend on the composition and rate of cooling, and may vary in a given composition between 3.5 and 8.0 percent. The crystallization of the solid solution between NC_8A_3 and C_3A in the form of prismatic crystals has suggested that these may explain the prismatic dark interstitial material. This phase will be discussed later. An observed enlargement of the primary-phase region of CaO, due to the addition of Na_2O to the system CaO–Al_2O_3–SiO_2, explains the increased difficulty of satisfactory burning with increases in the soda content of the mix.

3. Combinations in the System CaO—MgO—Al_2O_3—Fe_2O_3—SiO_2

In a recent paper by Swayze [38], three systems of immediate interest to an understanding of portland cement constitution have been reported. These are:

(a) CaO–C_5A_3–C_2F,
(b) CaO–C_5A_3–C_2F–C_2S, and
(c) CaO–C_5A_3–C_2F–C_2S plus 5 percent of MgO.

These will be considered separately.

(a) System CaO—C_5A_3—C_2F

In mixtures containing ferric oxide, difficulty has usually been experienced in obtaining satisfactory quenched charges due to the very rapid crystallization of the iron compounds. Swayze overcame this difficulty by using very small charges (0.002 to 0.015 g), placing these on open, concave platinum-foil containers, and quenching in water. By this means, charges containing up to 75 percent C_4AF could be completely frozen as glass.

It had been reported formerly [13] that C_2F forms a solid-solution series with a hypothetical C_2A up to a composition of C_4AF. As this was the end member of the series highest in alumina, and as cements nearly always contain alumina in excess of the amount that could thus combine with the available ferric oxide, the compound C_4AF was considered to be the stable iron-containing compound of portland cement. Swayze found, however, that the solid-solution series extends further towards the C_2A point, reaching an end member having the composition C_6A_2F. The Al_2O_3:Fe_2O_3 ration of C_6A_2F is 1.28 whereas that of C_4AF is 0.64. This means, therefore, that in portland cements having an Al_2O_3:Fe_2O_3 ratio above 1.28 the iron will be present (at crystalline equilibrium) in the form of C_6A_2F. And in cements having an Al_2O_3:Fe_2O_3 ratio between 1.28 and 0.64, the composition of the crystalline iron phase will have a composition between that of C_6A_2F and C_4AF. If the Al_2O_3:Fe_2O_3 ratio is below 0.64, the composition of the iron phase will lie between that of C_4AF and C_2F. According to the earlier studies, C_3A could appear as a separate phase from compositions having an Al_2O_3:Fe_2O_3 ratio in excess of 0.64, but from the new work this appears not to be possible until that ratio has exceeded 1.28.

718313—47——4

(b) System $CaO—C_3A_3—C_2F—C_2S$

The above study on the ternary system was extended into the quaternary system with silica by addition of the fourth component, C_2S. This was necessary in order to find the influence of the above phase relations on the formation of the calcium silicates. This system previously had been reported by Lea and Parker [26].

The principal interest here is concerned with the C_3S area and the invariant points of that phase with those adjacent to it. The work of Swayze shows excellent agreement with the earlier work in the temperatures of the invariant points $CaO—C_3S—C_3A—$iron phase and $C_3S—C_2S—C_3A—$iron phase. His compositions, however, are richer in iron and poorer in lime than the corresponding points of Lea and Parker. This appears to be of especial significance by bringing these invariant compositions outside the tetrahedron $C_3S—C_2S—C_3A—C_6A_2F$. This indicates that the iron phase that will be in equilibrium in the final products of crystallization of those compositions will belong to the solid-solution series.

(c) System $CaO—C_3A_3—C_2F—C_2S$ Plus 5 Percent MgO

As all portland-cement clinkers contain some magnesia, the study was continued with the introduction of 5 percent of MgO. This amount was added because it previously had been learned that liquids in the region under study, between Al_2O_3:Fe_2O_3 ratios of 1.35 and 1.60, take up slightly less than 5 percent of MgO at temperatures at which the C_3A and the iron phase have just disappeared. Saturation of the liquid was indicated by the presence of small amounts of periclase (MgO) in most of the glasses examined.

The effect due to the introduction of the MgO was found to be an increase of the Al_2O_3 content and a decrease in Fe_2O_3 and CaO, in both of the principal invariant compositions. This lengthens the field of the iron solid-solution phase and shortens that of the C_3A on the C_3S surface to such an extent that the invariant points are brought to the high-alumina side of the plane that passes through C_3S, C_2S and C_6A_2F. This brings these points within the tetrahedron $C_3S—C_2S—C_3A—C_6A_2F$, and makes possible the formation of C_6A_2F in the presence of C_3A, C_2S and liquid.

In these studies, it was shown that crystals of one phase might become embedded in another phase during crystallization of the latter and so prevent the theoretical course of crystallization, even at very slow cooling. Thus CaO, which under theoretical equilibrium would be resorbed, may be left free, enclosed in crystals of C_3A or C_3S. Furthermore, as the members of the solid-solution series are stable in the presence of each other, there may be practically no redistribution of Fe_2O_3 and Al_2O_3 within the growing crystals, which would be necessary under equilibrium cooling. This makes possible the formation of crystals having a low Al_2O_3:Fe_2O_3 ratio core and a higher Al_2O_3:Fe_2O_3 ratio exterior.

Swayze points out that the establishment of a solid-solution series ranging from C_2F to C_6A_2F may explain many anomalies that have been observed in the constitution of portland cement. Thus the petrographic examination of clinkers has usually shown an excess of C_3S and a deficiency of C_2S and C_3A from the amounts calculated on the assumption that the iron is completely in the form of C_4AF. If the iron goes into combination as C_6A_2F, more Al_2O_3 is taken into that compound, and less into C_3A. This leaves an excess of CaO to combine with C_2S, reducing the latter and increasing the C_3S. Likewise, the heat of solution of C_6A_2F may be expected to differ from that of C_4AF, and this would affect the calculated values for glass content as obtained by heat-of-solution methods.

Before closing this section of the paper, attention should be called to a recent contribution by Dahl [8] in which the interpretation of phase diagrams is considered. Of especial interest in connection with phase-equilibria studies on portland cement, methods are developed for determining the phases present at equilibrium at any given temperature, and for estimating their proportions, without tracing the course of crystallization from the liquid state. Attention is also given to the role of the liquid phase in the processes of fusion and crystallization, as a means of gaining an understanding of the mechanism by which the oxides in the raw materials are transformed into the various cement compounds.

4. Prismatic Tricalcium Aluminate

When polished and etched sections of clinkers are examined under the metallurgical microscope, there is often observed a dark interstitial material. This may occur in three forms. A rectangular

phase has been identified as $3CaO.Al_2O_3$, and an amorphous phase as glass [20]. A prismatic phase has been observed in many clinkers [19] but, when charges have been made from pure materials, only those containing K_2O or Na_2O have shown that phase. The optical properties of the prismatic phase, however, did not correspond with those of any of the known alkali compounds, nor has there been revealed any relationship between the percentage of alkalies in clinker and the amount of prismatic material observed [43]. There was seen, however, to be a close relationship between the *total* dark interstitial material and the potential C_3A content. The prismatic phase was found to be more abundant in clinkers that were cooled at an intermediate rate: when rapidly cooled, glass predominated, and when slowly cooled, the rectangular form predominated.

In a study looking to the solution of the problem, Taylor [42] selected a number of compositions in the system $KC_{23}S_{12}$–CaO–C_5A_3, and subjected them to a variety of heat treatments. The results of this study showed that, under equilibrium cooling, the prismatic form was not observed in any case. Under more rapid cooling the prismatic form appeared in those compositions in which C_3A was one of the compounds anticipated from the phase diagram [41]. If the charge were quenched from a temperature above that at which C_3A was formed, the prismatic phase was not found.

This study indicated that C_3A may separate from a mixture in three forms. When quenched above the temperature of crystallization, it will be glass, observed as an *amorphous* dark interstitial phase. When cooled slowly enough to attain equilibrium crystallization, it will appear as *rectangular* crystals. But when cooled at intermediate rates, it may separate in *prismatic* form. No methods appeared to be available for defining precisely the composition of that phase but, if it is a solid solution, the extent of such solution was shown to be very slight. The presence of K_2O and SiO_2 or Na_2O and SiO_2 appears to be essential to its formation, but the reason assigned is associated with the attainment in the crystallizing liquid of the proper environment for the production of a metastable phase.

From this study it is concluded that the prismatic dark interstitial material is a metastable form of tricalcium aluminate, monotropic with respect to the stable, isotropic, rectangular form of that compound.

5. Inversion of Dicalcium Silicate

The inversion temperature of α to βC_2S was reported in 1915 by Rankin and Wright [34] as 1420° ±2° C. In a study by Newman and Wells [32] on the effect of added materials on C_2S, the authors observed inconsistencies in heating- and cooling-curves that denoted that the earlier inversion-temperature value had been set too low. By the use of differential heating-curves, the points of energy-change could be established with a high degree of precision.

A standard sample of γC_2S was prepared from "low alkali" $CaCO_3$ (containing less than 0.042 percent total determined impurities), and a silica gel (0.06 percent residue nonvolatile with HF). A precisely proportioned mixture was heated for 1 hour at 1450°C, cooled, remixed, and the process repeated three times. A β–α inversion temperature of 1456°±2.2° C was obtained.

The addition of CaO up to 4 percent did not change the β–α inversion temperature, nor did the addition of 0.12 percent of SiO_2. But when 0.19 percent of SiO_2 was added, the inversion temperature was lowered to 1,438° C. Further additions of SiO_2 caused no further reductions. As these small variations in composition could not readily be detected by chemical means, the authors concluded that the inversion temperature of pure dicalcium silicate could be assumed to be 1,438° C (which would be raised to 1,456° C by the addition of a small amount of CaO), or 1,456° C (which would be lowered to 1,438° C by the addition of a small amount of SiO_2). The authors believe that the higher value more correctly indicates the true inversion temperature.

The authors then studied the effects due to the introduction of foreign oxides. The principle was followed that the inversion temperature is lowered when a foreign material is less soluble in the low-temperature form (as βC_2S) than in the high-temperature form (as αC_2S). After saturation is reached, no further temperature change takes place. Hence, by plotting inversion temperature against increasing concentration of solute added, the limiting solubility is noted as the concentration beyond which the inversion temperature remains sensibly constant. The solubilities of the mate-

rials added to C_2S and the corresponding lowerings in the inversion temperature, were reported and found to vary over a wide range, as shown in table 1.

TABLE 1.—*Solubility of oxides in αC_2S, and consequent lowerings in inversion temperature*

Oxide	Solubility in C_2S	Lowering in temperature of inversion point
		°C
Al_2O_3	0.5	14
MgO	.5	20
Fe_2O_3	1.0	20
CaF_2	.7	2
TiO_2	1.0	21
BaO	[1] 20	200
Cr_2O_3	2.5	61
V_2O_5	.5	29
P_2O_5	1.0	66
B_2O_3	8.0	151
Mn_2O_3	8.0	73
K_2O	1.6	54
Na_2O	[1] 1.3	166

[1] Limit not reached.

A study of the β to γ inversion of C_2S has been made by Zerfoss and Davis [46]. The effects were observed of the addition of oxides of P, As, Sb, V, Ba, Sr, Zn, Cr, W, Mo and Ti. These investigators found that the addition of 1 mole percent of P_2O_5, As_2O_5, V_2O_5, or Cr_2O_3 inhibited the inversion and allowed the β C_2S to be stable at room temperatures. It had long been known that B_2O_3 prevented dusting, and recent work by Newman and Wells [32] has shown that Mn_2O_3 likewise should be included.

In all cases, the optical properties of the C_2S were changed, which indicates the formation of a solid solution. Zerfoss and Davis conclude that the β-γ inversion can be inhibited in two ways: chemically through the formation of a solid solution, and physically through the restraining influence of surrounding phases. The solid solution does not invert because of the high energy requirement necessary to force out the dissolved ion and allow the silicate to assume the stable form. In physical inhibition, the surrounding phases restrain the beta form from expanding to the gamma form, and isolate the grains so as to disturb and block the inversion wave.

According to these authors, the inversion involves an increase in the coordination number of the calcium, and any means by which the low coordination of the calcium in β C_2S can be preserved will prevent inversion. Thus they argue that we may consider the operation of the inversion as a stage in the competition of calcium and silicon for oxygen. Hence, by inserting other highly-charged atoms into the silicate structure, they, with the silicon, will compete with the calcium for the oxygen and will assist in preserving *the low coordination* of the calcium.

IV. Crystal Structure

A few studies on the crystal structure of the cement compounds during the past five-year period are of particular interest.

1. Structure of Tricalcium Aluminate

The structure of C_3A has been examined by a number of investigators. From studies of X-ray diffraction patterns, Harrington [14] concluded that it was "pseudocubic" with a unit cell having $a_0=7.62$A. There were however a number of lines to which he was unable to assign cubic indices. The density indicated three molecules in the cell. Steele and Davey [37] reported that the cell was cubic, with $a_0=7.64$A. There were difficulties however in the suggested arrangements of the atoms. Lagerquist, Wallmark and Westgren [25] assigned to the compound a cubic cell with an edge of 15.22A, which would give 24 molecules per unit cell.

Data obtained by McMurdie [29] indicate a cubic unit cell with $a_0=15.24$A, which allow all of the observed lines to be indexed. The strong lines of the diffraction pattern are those of a body-centered cube, with $a_0=3.81$A, which were shown to be caused by an arrangement of metal atoms at or near the corners of 3.81A cubes. By comparison with the known structure of other compounds having similar lines, it was shown that no deductions were permissible concerning the arrangement of the oxygen atoms. It had previously been noted by Brownmiller [5] that X-ray diffraction patterns consisting of the strong lines of C_3A were obtained from various quickly cooled liquids in the area of portland cement, even from some compositions in which Al_2O_3 was not present. His explanation was that this material was a metastable phase which, on slower cooling, was transformed to the stable crystalline phases. McMurdie concluded from his studies that the pattern was due to submicroscopic quench growths of a metastable crystalline compound.

2. Structure of Dicalcium Silicate

An important series of studies has been reported by Bredig [3] that have clarified the crystal structure of the several forms of dicalcium silicate. A group of compounds (as K_2SO_4, Na_2SO_4, CaNaPO4, $CaKPO_4$) is represented by the general formula A_2XO_4. Although occurring in more than one modification, their high-temperature (α) forms are similar and show hexagonal symmetry. Bredig observed, however, that a number of other phases, formerly designated as compounds, showed this same crystal symmetry. Thus glaserite $K_3Na(SO_4)_2$, and the silica-phosphate $7CaO.P_2O_5.2SiO_2$ gave the simple crystal lattice of the αA_2XO_4 group. For this reason they are believed by Bredig to be solid solutions. In the first case, the solution would be of Na_2SO_4 in K_2SO_4; in the latter case, of $3CaO.P_2O_5$ in $2CaO.SiO_2$.

A similar structure obtained by Greene [10] with specially heat-treated mixtures of Na_2O and Fe_2O_3, or Na_2O and Al_2O_3, with C_2S led him to conclude that solid solutions had been formed of Na_2O, with Fe_2O_3 or Al_2O_3, in C_2S. The structure in both of these cases was that of the αA_2XO_4 group, which is offered as evidence that the C_2S in these preparations is in the α form. The conclusion of this study was that αC_2S has a hexagonal symmetry and is stable at some high temperature; that ordinarily it is impossible to prevent inversions during cooling, but that the presence of substances in solid solution may cause the α form to be retained at room temperatures. A slow cooling through the transition-temperature range, however, brings about the inversion, as noted by a change in symmetry and the appearance of the typically-twinned β form.

Furthermore, it appears that the components of the solid solution are less soluble in the β than in the α form of C_2S, and so separate during the inversion. This gives rise to the inclusions commonly observed in the C_2S crystals of commercial clinkers. Greene found the inversion temperature to be lowered by the solution: to 1,175° by the $Na_2O+Fe_2O_3$, and to 1,180° by the $Na_2O+A1_2O_3$. These results led to the conclusion that the crystals formerly described as α C_2S were in reality the β modification, the slight differences observed being due to solid solutions.

By a similar procedure, Bredig showed that the phases $27CaO.P_2O_5.12SiO_2$ and $K_2O.23CaO.12SiO_2$, which had been considered as compounds, have a structure corresponding to the β or low-temperature form of K_2SO_4. This indicates to Bredig that those compounds are solid solutions, the former of $3CaO.P_2O_5$ and the latter of $K_2O.CaO.SiO_2$ in $2CaO.SiO_2$. The symmetry of this hypothetical form of C_2S is lower than that of the α form but higher than that of β C_2S. Since these solid solutions have the structure of β K_2SO_4, it is assumed that pure C_2S must also possess this structure in some temperature range. This new form is designated by Bredig as α' C_2S. Its temperature of stability is believed to be immediately above the α'—β transition point (1,420° C according to Rankin and Wright, and 1,456° C according to Newman and Wells, see above), and that of α C_2S to range from the α—α' transition point (undetermined) up to the melting point of C_2S.

The work of Bredig led to further developments on the relative activities of the various forms of dicalcium silicate. Brandenberger [2] had advanced the theory that the calcium ion at room temperature tends to surround itself with more oxygen ions than at high temperatures. Thus the coordination number of Ca for O in γC_2S is believed to be 6, but for the βC_2S, stable at higher temperatures, it is considered to be less than that value, and is set at 4. If this is true, an increased activity results upon a decrease in coordination number of CaO_6 to CaO_4. This theory was advanced on the premise that, with rising temperatures, the Ca ions exert a loosening influence upon the state of polarization of the O ions, increasing the distance between them and the Si ions, and so diminishing the bond between them. Such action was called "contrapolarization."

Bredig argues against the possibility of this effect with rising temperature. On the contrary, he contends that it is at low heat contents that the weaker Ca cation may approach the SiO_2 radical close enough to exert increased attraction upon the electron shell of the O ions, and be able thereby to repulse the Si ions. Hence, he argues, if the coordination number of Ca for O in γC_2S is 6, as there is reason to believe, the number will increase in the polymorphic forms stable at the higher temperatures. He places the value in the α and α' forms at about 10, and in the β form at an intermediate value, probably 8.

In justification for this assumption, Bredig

points out that, in $Ca(OH)_2$, the Ca ion establishes around itself a shell of 6 oxygen ions. In γC_2S, where the shell already consists of CaO_6, there is no potential to afford the chemical exchange in reaction with water. Hence γC_2S is unreactive towards water. But in the case of the unstable coordination CaO_8 of the βC_2S, the tendency to revert to CaO_8 may be so great that the change in free energy may account for the activation energy of interaction with water.

The assumption of a hexagonal form of C_2S, stable at a temperature above the transition temperature, has recently been confirmed by McMurdie and van Valkenburg [31]. Making use of a specially-designed furnace, in connection with a Phillips X-ray spectrometer (which employs a Geiger counter in place of a photographic film), the diffraction pattern was obtained on a specimen at about 1,500° C, and the hexagonal structure noted.

V. Reactions of Hydration

In the field of the hydration of the cement compounds, important advances have currently been made along several directions.

1. System CaO-Al_2O_3-H_2O

A recent study of much interest has been made by Wells, Clarke, and McMurdie [44] on the system CaO-Al_2O_3-H_2O at 21° and at 90° C. Metastable solutions of calcium aluminates were prepared by shaking for an hour or so either anhydrous calcium aluminates less basic than C_3A, or alkali-free calcium aluminate cements, with distilled water in the proportion of 50 g per liter. These mixtures were filtered, and clear solutions obtained containing up to 2.4 g of Al_2O_3 and 1.4 g of CaO per liter. Portions were then mixed with solutions of $Ca(OH)_2$ of known concentrations and the changes in the solution observed.

It was noted that increases in CaO content of the solutions were accompanied by decreases in Al_2O_3 content, and a gradual increase from 2 to 4 in the molar ratio $CaO:Al_2O_3$ in the solid phases. This latter effect could be due either to an overlapping of the solubility curves of a series of separate hydrated aluminates, or to the solubility curve of a solid-solution series of varying $CaO.Al_2O_3$ ratio. The problem could not be solved by the examination of the optical properties of the crystals, because the individual crystals were too small for satisfactory interference figures. Refractive indices were not greatly different between crystals of low lime content ($2CaO.Al_2O_3.5$–$9H_2O$) and those of high lime content ($4CaO.Al_2O_3$.-12–$14H_2O$), but the so-called ω index of the dibasic compound was somewhat lower than that of the tetrabasic compound. The crystals of $4CaO.Al_2O_3.12H_2O$ were found to be biaxial negative, with indices $\gamma=1.542$, $\beta=1.538$ and $\alpha=1.522$.

The metastable invariant point for C_2AH_8 and C_4AH_{13} was found to lie between 0.5 and 0.6g of CaO per liter, and between 0.10 and 0.15 g of Al_2O_3 per liter. At lower lime concentrations, the 2:1 compound predominated; at higher lime concentrations the 4:1 compound predominated. The X-ray diffraction patterns of both preparations show a hexagonal unit cell in which $a=8.8A$ The value of c for the 2:1 compound was 10.6A, and for the 4:1 compound was 8.2A. The patterns for the crystals of intermediate composition gave intensities that indicated a mixture of C_2AH_8 and C_4AH_{13}.

From these observations, Wells and his associates concluded that the so-called hexagonal tricalcium aluminate hydrate is in reality not a separate compound but a mixture of the hexagonal hydrated C_2A and C_4A in equal molar proportions. The similar structure of these compounds parallel to the a axis led to the belief that they are capable of intercrystallization, and are made up of layers of the one compound so intimately mixed with layers of the other that the average indices of refraction are obtained.

Specimens stored in sealed vials for 2 to 3 years showed an increase in refractive indices in the low-lime compositions to values similar to those of the high-lime compositions, and the X-ray patterns in all cases were those of the 4:1 compound. This indicated that the 2:1 compound is unstable and decomposes to the 4:1 composition.

At temperatures above 21° C, the hexagonal forms were found to revert rather slowly to the isometric C_3AH_6, and the solubility of the stable compound increased up to 90° C. From observations on the formation of hydrated alumina in some preparations, it was concluded that gibbsite ($Al_2O_3.3H_2O$) is the stable phase in the system CaO–Al_2O_3–H_2O at 21° C up to a concentration of 0.33 g of CaO per liter, and that isometric

C_3AH_6 is the stable phase above that concentration between 21° and 90° C. The liquid at the invariant point for C_3AH_6–AH_3 contains 0.02 g of Al_2O_3 per liter at 21° C and 0.11 g of Al_2O_3 per liter at 90° C.

It was found by Harris, Schneider, and Thorvaldson [15] that, although the isometric C_3AH_6 is the stable phase in the temperature range around 150° C, a prolonged treatment in steam at nigher temperature results in the formation of birefringent crystalline phases. At temperatures below 200° C, the mean refractive index of this material was 1.58. Between 205° and 350° C, rectangular prismatic plates were formed with a $CaO:Al_2O_3$ ratio less than 1.5, as well as $Ca(OH)_2$, but no free hydrated alumina. Two of the refractive indices of the crystalline hydroaluminate were close to 1.627.

This work indicates that, under conditions favoring hydrolysis, one and possibly two birefringent hydroaluminates may be formed: one at a temperature of about 200° C having a mean index of 1.58 and one at higher temperatures having an index of 1.627. It was suggested that the formation of these birefringent hydroaluminates may be an important factor in the improvement of sulfate resistance of cements subjected to steam curing.

2. The Setting Process

The character of the hydrated calcium silicate that was formed in systems of cement components with water was investigated by Hedin [16]. When 0.2 g portions of C_3S or βC_2S were shaken with liter quantities of water, the compounds entered the solution in the molecular proportions of the anhydrous compounds. But after about 24 hours, in the case of the C_3S, a cotton-like precipitate formed having the composition CSH. In more basic solutions the reaction was different. When 500 ml of the C_3S solution was added to 2 liters of saturated lime water, the precipitate that formed had the composition C_2SH_4. An X-ray examination showed the material to be crystalline. A number of additional experiments led Hedin to believe that this hydrate is the normal silicate compound formed during the hydration of cement.

The rate of the reaction was found to be affected greatly by the presence of other ions in the solution. Thus the reaction with either C_3S or C_2S is greatly depressed by saturated solutions of $Ca(OH)_2$, but to a less degree when gypsum is present with the $Ca(OH)_2$. Still less depression is caused by a 5 percent solution of $CaCl_2$ in the lime water.

On working with the calcium aluminates, Hedin found that these compounds entered into solution congruently when the concentrations were very low. As with the calcium silicates, the rate of solution was found to be greatly depressed in saturated solutions of $Ca(OH)_2$, but to an even greater extent when gypsum was also present. Rapid reaction prevailed in those solutions in which quick set occurred, whereas the reactions were slow and the solubility low in solutions where the set was normal. In the latter case, the reaction appeared to be depressed due to a coating of the grains with an insoluble film of a hydration product that hindered the penetration of the solution.

Thus Hedin found that the concentration of the calcium ions in the solution affects to an important degree the solubility of both the silicate and the aluminate anhydrous compounds, but the basicity of the solution affects only the aluminates. The systematic control of these factors would permit the control of the setting process as well as many other properties that are dependent upon the character of the set. Thus gypsum accelerates the solution of the calcium silicates but retards the solution of the calcium aluminates. The pH may be so greatly reduced by some calcium salts, as $CaCl_2$, that precipitation of the calcium aluminate is prevented entirely, and in its place $Al(OH)_3$ may be formed. Even the composition of the hydrated calcium silicate may be changed, from C_2SH_4 in supersaturated lime solutions to $C_3S_2H_x$ in saturated lime solutions.

When quick set occurs, there is a mutual coagulation of the silicic acid and aluminum hydroxide, enclosing unhydrated grains and impairing strength. If the lime can be brought into solution rapidly, this coagulation is prevented by the prior formation of C_4A hydrate. The silicate can then hydrate unaffected by the aluminate. Gypsum would give an effect similar to the lime, due to the prior formation of insoluble calcium sulfoaluminate.

The question of set has been studied by Lerch [27], making use of a conduction calorimeter for indicating the rate and extent of heat liberation. Two or three cycles of increasing heat liberation were found for all cements. The first cycle appears rapidly after mixing with water, and is

explained as due to the initial rapid solution of the anhydrous aluminates. During this period, lime and gypsum are going rapidly into solution and in a few minutes normally reach such a concentration that the first reactions are depressed through a sharp decrease in the solubility of the alumina in such solution. This results in a decrease in rate of heat liberation.

When the solution has become saturated with lime, the aluminates continue to dissolve slowly and react with gypsum to form calcium sulfoaluminate. The silicates dissolve and form hydrated calcium silicates. These reactions increase to the time of initial set, following which a slowing down occurs due to film formation of hydration products around unhydrated material and to the disappearance of the smaller grains. When the gypsum has become depleted, the SO_3 concentration in the solution drops sharply, resulting in an accelerated solution of the aluminates and increase in heat evolution.

The rate and time of the above reactions are determined by the composition and fineness of the cements. With low C_3A and low alkali, the reaction is slow and is accelerated by gypsum. Alkalies bring about a more rapid reaction, and require a higher gypsum content for proper retardation. Thus it appeared to Lerch that each cement has a gypsum requirement for optimum retardation that is characteristic of its composition and fineness. Tests on strength, expansion in water and contraction in air all indicated that the best results are obtained when this optimum amount of gypsum is present. This optimum quantity is defined by Lerch as the minimum amount of gypsum that will give a heat-liberation curve showing two cycles of ascending and descending rates, and showing no appreciable change with larger additions of gypsum.

A convenient test for the maximum SO_3 content was devised that was based on the concentration of SO_3 in neat cement pastes at 24 hours. If the pastes retain gypsum, the SO_3 concentration of the extracts will approach that of saturated gypsum which is 1.2 g per liter. If the gypsum has been depleted, the SO_3 concentration will approach that of calcium sulfoaluminate, which is about 0.05 g per liter. The maximum amount of gypsum permissible in the cement, according to the theory underlying the test, should be such that no or very little unreacted gypsum shall remain in the specimen of paste at 24 hours, and hence the SO_3 in the extract should be of the lower order of magnitude.

Confirmation of the results of Lerch was obtained by Whittaker and Wessels [45]. They found that many cements required larger amounts of gypsum than were allowed by the standard specifications, varying between 3 and 4 percent of SO_3, to retard properly the rates of hydration. By the use of the larger percentages of gypsum, little effect was noted on time of set, but improvements were observed by a reduced autoclave expansion and increased tensile and compressive strengths, especially at early ages. An increased tendency to a false set with the higher-SO_3 cements was noted, especially when grinding temperatures were high.

Calcium chloride was found by Lerch to accelerate the hydration of cement pastes, as indicated by an increase in heat liberated during the first few hours and a shifting of the peak of maximum heat liberation to an earlier age. This would be reflected in an earlier set and increased strength at early ages. Kalousek, Jumper, and Tregoning [24] noted that $CaCl_2$ differed in its action from $CaSO_4$ by bringing about in the pastes an increase in the alkalies dissolved. This was thought to accelerate the precipitation of calcium sulfoaluminate (and perhaps also of calcium chloraluminate) and so to lower the concentration of CaO and SO_3 in the solution.

An acceleration of hydration was also found by Lerch when K_2SO_4 or Na_2SO_4 were added to the solution. This was explained as due to an interaction of the alkali sulfates with calcium hydroxide.

3. Hydroaluminate Complex Salts

The action of gypsum in the retardation of set, and the action of sulfate waters on concrete, can be understood only by a knowledge of the compounds and reactions in the system C_3A–$CaSO_4$–H_2O. The formation of a calcium sulfoaluminate was known to Candlot [7] as early as 1890, and many investigators have contributed to our information. In addition to a high-sulfate form ($C_3A.\ 3CaSO_4.\ 31H_2O$, which will be referred to as the "trisulfate") a low-sulfate form ($C_3A.\ CaSO_4.\ 12H_2O$) was discovered (referred to as the "monosulfate") [28]. The trisulfate was found to be the more stable and the only form observed in cement

paste after reaction with sulfates. Its solubility being very low and its formation aided by the presence of $Ca(OH)_2$, it formed readily in cement pastes.

The monosulfate was found by Kalousek [22] to be metastable in solutions throughout a wide range of composition, but to persist over long periods in the absence of an excess of sulfate. With increasing concentrations of alkali hydroxide in the solution, the molar ratio of SO_3:Al_2O_3 of the crystals was found to decrease, so that the trisulfate could not exist at NaOH concentrations above 0.25 equivalents per liter. While the SO_3:Al_2O_3 ratio varied between 0.68 and 0.22, the CaO:Al_2O_3 ratio remained at about 4. These results led to the belief that a solid-solution series was formed between $C_3A.CaSO_4.12H_2O$ and $C_3A.Ca(OH)_2.13H_2O$, and between the tri- and monosulfate. This series could be expressed:

$$\begin{array}{ccc} C_3A.3Ca(OH)_2.xH_2O & — & C_3A.3CaSO_4.31H_2O \\ | & & | \\ C_3A.Ca(OH)_2.13H_2O & — & C_3A.CaSO_4.12H_2O \\ & & | \\ & & C_3A.12H_2O \end{array}$$

The conversion from mono- to trisulfate was found to be accompanied by an increase in volume that could explain undesirable expansions in concrete subjected to sulfate waters.

Flint and Wells [9] prepared compounds analogous to the calcium sulfoaluminates, containing $CaSiO_3$ or $Ca(OH)_2$ in place of $CaSO_4$. The relationship between these and the corresponding sulfoaluminates may be represented as follows:

$$C_3A \left\{ \begin{matrix} CaSO_4 \\ CaSiO_3 \\ Ca(OH)_2 \end{matrix} \right\} 12 \text{ to } 13H_2O$$

$$C_3A \left\{ \begin{matrix} 3CaSO_4 \\ 3CaSiO_3 \\ 3Ca(OH)_2 \end{matrix} \right\} 31H_2O$$

It was suggested that the complex sulfoaluminates hydrate known to be formed in cement pastes might vary in composition because of partial replacement of the sulfate radical by either the hydroxyl or the silicate radical in a solid-solution series.

A noteworthy attempt to resolve the systems quantitatively has been made by Jones [21]. Examining the system CaO-Al_2O_3-$CaSO_4$-H_2O at 25° C, Jones found the trisulfate to be the only stable complex salt that was formed. The monosulfate, however, was found to be a possible metastable phase that might be formed as the end member of a solid-solution series. An abrupt increase in Al_2O_3 occurred at a CaO concentration of about 0.3 g of CaO per liter, and the $CaSO_4$ concentration became very small. The solid phase then had a composition close to the monosulfate, but with increasing CaO concentrations the composition moved toward $C_3A.Ca(OH)_2.12H_2O$.

In such solutions (free of alkali and iron), Jones concludes that the complex salt first formed is the trisulfate, but that this may change over partially or completely into the metastable solid solution, to which he assigns the formula xCaO.$y$$Al_2O_3$.$z$$CaSO_4$.aq. The explanation given is that the solution becomes rapidly supersaturated with respect to $Ca(OH)_2$ and, as long as solid gypsum remains, an equilibrium will be maintained between the trisulfate, calcium hydroxide and gypsum. When the gypsum is used up, C_3AH_6 should form under stable equilibrium, but that compound is slow to form and the system is more likely to pass to the metastable region where the solid solution appears. In this way Jones thinks that, with a cement containing 2 percent of SO_3 and 2.6 percent or more of Al_2O_3, complete conversion of the trisulfate to the solid solution is possible.

When KOH or NaOH were added to the system in amounts of 1 percent, there resulted a greatly increased solubility of alumina and a greatly decreased solubility of lime. But still the trisulfate was the only stable complex salt observed. These results differ from those of Kalousek, who found the monosulfate solid solutions to be stable above certain NaOH concentrations. This may be accounted for by the use, by Kalousek, of higher NaOH concentrations than used by Jones. Kalousek's results differed from those of Jones in that he failed to find C_2AH_6 in any of the solid phases.

VI. New Technics

A number of new technics, resulting from the use of special equipment, have recently been applied in cement research, and merit a brief mention.

1. Methods of Spectrographic Analysis

Methods have recently been developed by Helz [17] and by Helz and Scribner [18] by which eight elements may simultaneously be determined spectrographically in portland cement. These elements are sodium, potassium, lithium, magnesium, manganese, titanium, iron, and aluminum. A number of items of technic may be mentioned. The most satisfactory sample consists of a compressed pellet containing a mixture of the cement, graphite, and cobalt oxide in proper proportions. The graphite was found necessary for the smooth burning of the charge in the electrode, and the cobalt oxide is employed as the internal standard. The disk-shaped pellet (½ in. in diameter by ⅛ in. thick) is used as the lower electrode. A "multisource" power unit employing an overdamped condenser discharge was found to give best results.

It has been found that potassium interferes with the determination of sodium, but that the magnitude of such interference changes very little when the concentration of K_2O varies between 1 and 2 percent. The difficulty was overcome by adding 0.7 percent of K_2O, as KNO_3, to all samples and, in the calculation, reducing by that amount the K_2O observed to be present.

By this procedure it was found to be possible for one operator to determine in duplicate in one day the above eight elements on 10 to 16 cements. The accuracy is probably as good as, or better than, that obtained by the usual chemical methods of analysis. The probable errors, expressed as percentages of the concentrations, are between 2 and 5 percent, except for potassium for which the error is about 8 percent.

2. Electron Microscopy

Another recent tool that offers possibilities of much interest in cement research is the electron microscope. By means of this instrument, micrographs may be obtained at magnifications up to 25,000 diameters with high resolution (which may subsequently be many times enlarged), and electron diffraction patterns may be photographed.

In the last few years, the instrument has been applied successfully to many problems requiring resolution of fine structure. In the field of portland cement, Eitel and his coworkers [33] have examined the hydration products of tricalcium silicate and tricalcium aluminate. More recently Katz and his associates [35] have reported the electron-micrographs of hydrated portland cements as also of some of the cement compounds. By this means Eitel found C_3S to give rise to hemispheres of $Ca(OH)_2$ and nodules identified as a calcium hydrosilicate. The C_3A gave hexagonal crystals identified as C_3AH_{12} and isometric crystals of C_3AH_6. Katz observed from C_3S and C_2S rhombic slabs (probably $CaCO_3$) and amorphous spherulites, and from C_3A the same rhombic slabs, thin hexagonal plates and spherulites. When a sulfate was present, needles and splines of calcium sulfoaluminate were observed.

Electron micrographs of the cement compounds made by McMurdie [30] showed no evidence of the rhombic slabs observed very commonly by Katz. The C_3A yielded hexagonal plates, as did also C_4AF and NC_8A_3. The C_3S and C_2S, as well as commercial cements, showed the presence of globules of gel, with fringes that suggest a possible beginning of crystallization. In the presence of gypsum, with C_3A or C_4AF, the heavy splines of calcium sulfoaluminate were conspicuous.

The above results are only the first pioneer work, which indicates that the electron microscope is adaptable to the examination of cement hydration products. The field of its application to the problems of cement research lies in the future. The use of electron diffraction technic has not been probed, but there is the probability that this also may be very useful. By this means the formation of solid solutions may be indicated, patterns of the several phases in a section may be separately obtained, and advantage may be taken of the opacity of thin films to electrons by applying the method to such films of hydration products formed on anhydrous crystals.

3. X-Ray Spectrometry

The present availability of an X-ray spectrometer (Phillips), employing a Geiger counter in place of a photographic film, makes possible the recording upon a chart both the intensity and spacings of the diffraction lines of a pattern. A photometer is not necessary for measuring the density of the lines, as intensity is indicated directly, and the spacings have only to be read from the chart.

Many advantages are possible from the use of this instrument. The examination of a specimen

is possible in a much shorter space of time, and there are no films to be developed. The unique possibility presents itself of placing the sample in a small furnace inserted in the instrument, so that the X-ray pattern of materials at high temperatures may be determined. Such a furnace has been successfully built and operated by McMurdie and van Valkenburg [31] at the National Bureau of Standards. Its use may be of the highest importance in studies on the crystal structure of compounds, inversion temperatures and solid solutions. The field has only been indicated; its exploration lies in the future.

VII. Summary

The foregoing may be summarized as follows: (1) The stable potash compound (or solid solution) in a cement mixture consisting of K_2O, CaO, MgO, Al_2O_3, Fe_2O_3, and SiO_2 has the composition $KC_{23}S_{12}$. When SO_3 is present, the potash combines with it preferentially to form K_2SO_4. (2) The soda of cement, in a mixture consisting of Na_2O, CaO, Al_2O_3 and SiO_2 may crystallize in the form of NC_8A_3, or a solid solution of that phase in C_3A; a solid solution of a soda-bearing phase in αC_2S; or inclusions of a soda-bearing phase in βC_2S. (3) The iron-bearing phase in portland cement is a solid solution of C_2F in a hypothetical C_6A, which may extend beyond the composition C_6AF, and reach an end composition at C_6A_2F. (4) The prismatic dark-interstitial phase of clinker is a metastable form of tricalcium aluminate possibly containing a small amount of alkali in solid solution. (5) The $\alpha-\beta$ inversion temperature of dicalcium silicate is probably 1,456° C. (6) The $\beta-\gamma$ inversion of dicalcium silicate may be prevented by 1-mole percent additions of P_2O_5, As_2O_3, V_2O_5, Cr_2O_3, B_2O_3, or Mn_2O_3. (7) Tricalcium aluminate has a cubic unit cell having a_0=15.24A and 24 molecules. (8) αC_2S has a hexagonal symmetry, stable at a high temperature. Under proper conditions, this may be obtained at low temperature. Previously described αC_2S is βC_2S, whose twinning is caused by the inversion and whose inclusions are the result of ex-solution of dissolved phases. (9) An $\alpha' C_2S$ exists, having the structure of βK_2SO_4. It is stable between the stability range of the α and the β forms. (10) Hexagonal C_3A-hydrate does not exist. The material previously designated as such is a mixture of C_2A aq and C_4A aq. (11) In steam at temperatures above 200° C, the isometric C_3AH_6 is changed into birefringent phases of two forms. (12) Supporting evidence is given in favor of the film theory to account for the reactions of set. (13) Each cement has a gypsum requirement for optimum retardation that is characteristic of the cement. (14) Calcium sulfoaluminate forms a series of solid solutions of high and low sulfate content, and the sulfate may be progressively replaced by hydroxyl or silicate. (15) Spectroscopic methods are developed by which 8 elements may be determined in duplicate on 10 to 16 cements by one operator in one day. (16) Methods of electron microscopy and X-ray spectrometry show promise of useful application in cement research.

VIII. References

[1] R. H. Bogue, The chemistry of portland cement (Reinhold Publishing Co., New York, N. Y., 1947).

[2] E. B. Bradenberger, Symposium on the chemistry of cements, p. 122 (Stockholm, 1938).

[3] M. A. Bredig, J. Phys. Chem. **46,** 474, 801 (1942); **47,** 587 (1943); **49,** 537 (1945); Am. Mineralogist **28,** 594 (1943).

[4] L. S. Brown. Unpublished data.

[5] L. T. Brownmiller, Am. J. Sci. **29,** 260 (1935); PCAF Paper 30; Am. J. Sci. **35,** 24 (1938); PCAF Paper 35.

[6] L. T. Brownmiller, R. H. Bogue, BS J. Research **8,** 289 (1932) RP414; Am. J. Sci. **23,** 501 (1932); PCAF Paper 25.

[7] E. Candlot, Bull. soc. encour. ind. nat., p. 682 (1890).

[8] L. A. Dahl, J. Phys. Chem. **50,** 96 (1946).

[9] E. P. Flint and L. S. Wells, J. Research NBS **33,** 471 (1944) RP1623.

[10] K. T. Greene, J. Research NBS **32,** 1 (1944) RP1570; PCAF Paper 45.

[11] K. T. Greene and R. H. Bogue J. Research NBS **36,** 185 (1946) RP1699; PCAF Paper 47.

[12] W. C. Hansen and R. H. Bogue, Ind. Eng. Chem. **19,** 1260 (1927); PCAF Paper 10.

[13] W. C. Hansen, L. T. Brownmiller, and R. H. Bogue, J. Am. Chem. Soc. **50,** 396 (1928); PCAF Paper 13.

[14] E. A. Harrington, Am. J. Sci. **13,** 467 (1927); PCAF Paper 8.

[15] G. M. Harris, W. G. Schneider, and T. Thorvaldson, Can. J. Research **21,** 65 (1943).

[16] R. Hedin, Proc. Swedish Cement Concrete Inst. **3** (1945).

[17] A. W. Helz, J. Research NBS **24,** 129 (1945) RP1633; PCAF Paper 46.

[18] A. W. Helz and B. F. Scribner, J. Research NBS **38,** 439 (1947) RP1786.

[19] H. Insley, E. P. Flint, E. S. Newman, and J. A. Swenson, J. Research NBS **21,** 355 (1938) RP1135.

[20] H. Insley and H. F. McMurdie, J. Research NBS **20,** 173 (1938) RP1074.

21] F. E. Jones, Trans. Faraday Soc. **35,** 1484 (1939); J. Phys. Chem. **48,** 311, 356, 379 (1944); **49,** 344 (1945).
[22] G. L. Kalousek, Univ. of Maryland Dissertation (1941); J. Am. Concrete Inst. **37,** 692 (1941) J. Phys. Chem. **49,** 405 (1945).
[23] G. L. Kalousek, C. H. Jumper, and J. J. Tregoning, Rock Products (April 1941).
[24] G. L. Kalousek, C. H. Jumper, and J. J. Tregoning, J. Research NBS, **30,** 215 (1943) RP1530.
[25] K. Lagerquist, S. Wallmark, and A. Westgren, Z. Anorg. allgem. Chem., **234,** 1 (1937).
[26] F. M. Lea and T. W. Parker, Phil. Trans. Royal Soc., **234,** No. 731, [A] 1 (1934).
[27] W. Lerch, Proc. Am. Soc. Testing Materials, **46,** (1946). In press.
[28] W. Lerch, F. W. Ashton, and R. H. Bogue, BS J. Research **2,** 715 (1929) RP54; PCAF Paper 19.
[29] H. F. McMurdie, J. Research, NBS **27,** 499 (1941), RP1437.
[30] H. F. McMurdie. Unpublished data.
[31] H. F. McMurdie and A. van Valkenburg. In preparation.
[32] E. S. Newman and L. S. Wells, J. Research NBS **36,** 137 (1946), RP1696.
[33] O. E. Radezewski, H. O. Muller, and W. Eitel, Naturwiss., **27,** 807, 837 (1939).
[34] G. Rankin and F. E. Wright, Am. J. Sci., **39,** 1 (1915).
[35] C. M. Sliepcevich, L. Gildart, and D. M. Katz, Ind. Eng. Chem. **35,** 1178 (1943).
[36] T. E. Stanton, Proc. Am. Soc. Civil Eng. **66,** 1781 (1940).
[37] F. A. Steele and W. P. Davey, J. Am. Chem. Soc. **51,** 2283 (1929).
[38] M. A. Swayze, Am. J. Sci. **244,** 1; 65 (1946).
[39] W. C. Taylor, J. Research NBS **21,** 315 (1938), RP1131; PCAF paper 37.
[40] W. C. Taylor, J. Research NBS **27,** 311 (1941), RP1421; PCAF Paper 40.
[41] W. C. Taylor, J. Research NBS **29,** 437 (1942), RP1521· PCAF Paper 43.
[42] W. C. Taylor, J. Research NBS **30,** 329 (1943), RP1536; PCAF Paper 44.
[43] G. W. Ward, J. Research NBS **26,** 49 (1941), RP1358; PCAF Paper 39.
[44] L. S. Wells, W. F. Clarke, and H. F. McMurdie, J. Research NBS **30,** 367 (1943), RP1539.
[45] A. G. Whittaker and V. E. Wessels, Rock Products, p. 95 (Aug. 1945).
[46] S. Zerfoss and H. M. Davis, J. Am. Ceramic Soc., **26,** 302 (1943).

WASHINGTON, March 24, 1947.